

R & D of SUPERCONDUCTING CAVITIES at K E K *

Kenji SAITO, Yuzo KOJIMA, Takaaki FURUYA, Shinji MITSUNOBU,
Shuichi NOGUCHI, Kenji HOSOYAMA, Toshiharu NAKAZATO¹,
Tsuyoshi TAJIMA, Kiyomitsu ASANO

KEK, National Laboratory for High Energy Physics
1-1 Oho, Tsukuba-shi, Ibaraki-ken, 305 Japan

Keigo INOUE, Yohsuke IINO

Mitsubishi Heavy Industries, Ltd., Nagoya Aircraft works
10, Oye-cho, Minato-ku, Nagoya, 455 Japan

Hirotoishi NOMURA

Nomura Plating, Co., Ltd.
5-12-20 Himejima, Nishiyodogawa-ku, Osaka, 555 Japan

and

Koichi TAKEUCHI

Tokyo Denkai, Ltd.
1-3-20 Higashisuna, Kohtoh-ku, Tokyo, 136 Japan

Abstract

We completed vertical tests of the TRISTAN scc during this spring, 1989. An accelerating field of 9.6 MV/m, Q_0 at 5 MV/m of 2.8×10^9 (on average) was obtained during these tests. Thus, a technical background has been established for scc large-scale applications to accelerators. In this paper, the R & D of surface treatment and niobium material at KEK is described, especially regarding the type of problems encountered and how they could be solved. Our technical level regarding large-scale scc production is also discussed.

1. Present Address: Laboratory of Nuclear Science, Tohoku University
1-2-1 Mikamine, Taihaku-ku, Sendai, 982 Japan

* Work supported in part by the US-Japan Collaboration Program

1. Introduction

The fabrication and vertical testing of thirty-two 508-MHz niobium five-cell cavities (TRISTAN scc) were completed this spring. The first sixteen cavities were installed in the TRISTAN Main Ring (MR) tunnel last summer. The energy of TRISTAN has been upgraded from 28.5 to 30.7 GeV. So far, the cavities have been working well at an average accelerating field gradient of 4.4 MV/m used for 3100 hours of physics runs. In addition, we installed the last sixteen cavities in MR one week before this workshop. The TRISTAN scc is the first large-scale application of superconductivity cavities in a storage ring. In this fabrication we obtained a maximum accelerating field (E_{accmax}) of 9.6 MV/m (on average) during vertical tests. The average Q_0 value at 5 MV/m was 2.8×10^9 . All of them passed our target values ($E_{accmax} > 5$ MV/m, $Q_0 > 2 \times 10^9$) sufficiently. Especially two-thirds of them reached an E_{accmax} of 10 MV/m.

We have been conducting R & D on 500-MHz niobium superconducting cavities (scc) for TRISTAN MR since '79. To make the description in this paper clear, we note here the history of our R & D (Fig.1).

From '80 to '82, we made one single-cell cavity every year and investigated the fabrication process with good reproducibility of scc performance. The fabrication method used consisted of spinning, heat treatment, electropolishing (EP) and oxipolishing and was established during this term [1].

In '83, three single-cell cavities were made. After measurements, they were joined with a three-cell structure at the end of this year. This cavity was the first multi-cell cavity and was beam tested twice in the TRISTAN Accumulation Ring (AR) during the end of May and during the beginning of July, '84. In these beam tests, the E_{accmax} was 4.3 MV/m and electron beam was accelerated to 5.2 GeV by using only the multi-cell cavity. Many encourag-

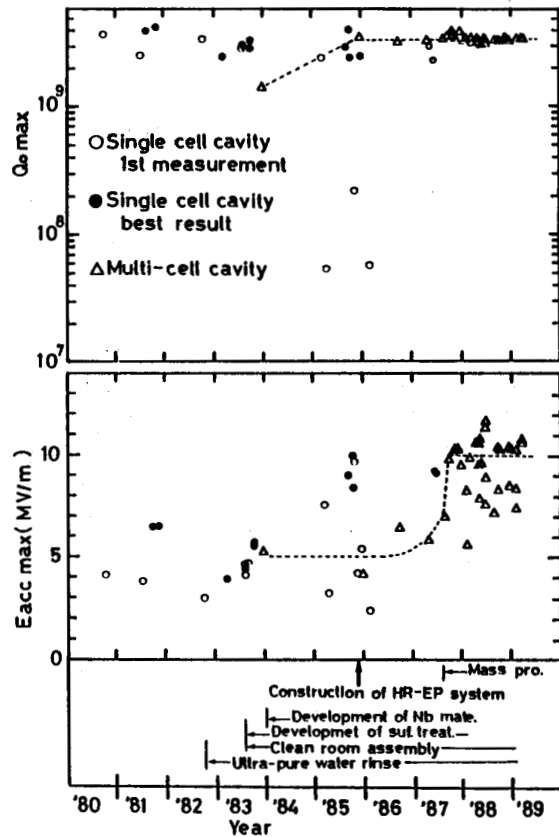


Fig.1
Development of 500-MHz scc at KEK.

ing results were obtained and the feasibility of scc application to MR was shown successfully [2] . However, one problem concerning the surface treatment was found: in multi-cell cavities high Q_0 values could not be obtained by the same electropolishing method as used in single-cell cavities [3] . Thus, since then, we have made efforts to develop an electropolishing method which is suitable for multi-cell structures.

From '84 to '85, we fabricated seven single-cell cavities. Five of them were joined with a five-cell structure (AR-#0) during the end of '85, and feedbacks from the above-mentioned EP studies were made to the fabrication. Furthermore, while starting to think of TRISTAN scc large-scale production, we tried to modify the fabrication process into a more simple one. These trials caused us to encounter problems; scc performance was scattered widely regarding both Q_0 value and E_{accmax} (Fig.1). However, they also educated us and played important roles during the construction of a reliable surface treatment system for the TRISTAN scc. During the end of '85, a horizontal rotational electropolishing (HR-EP) system was developed in order to solve the problems with the multi-cell EP. It was applied with a final EP of AR-#0. Although this method has not yet improved the accelerating field gradient(E_{acc}), it solved the low- Q_0 value problem in the multi-cell cavity.

On the other hand, during this term we became interested in niobium material from the view points of material quality control and high thermal conductivity. It was shown by H.Padamsee that the use of high thermal conductivity niobium could improve E_{acc} [4] . We made many efforts to develop a high thermal conductivity niobium material.

From '86 to '87, we made two five-cell cavities (AR-#1,2) which were planed to operate in AR. For the TRISTAN scc, we had to select a surface treatment process which was cheap as well as reliable. The HR-EP method made it possible to electropolish a completed multi-cell structure. It was possible to replace the heavy electropolishing of half cells by HR-EP. It was expected that electropolishing would become very simple and cheap by HR-EP. We checked the feasibility of using HR-EP in heavy electropolishing. In addition, in order to save the cost of waste disposal of EP solution, we tried to electropolish the cavities with used solutions during the final EP. However, the trial did not succeed. The E_{acc} of the cavities was limited to about 6 MV/m, due to surface contamination after using the EP solution.

Before going to large-scale production, we had to make a final choice regarding the fabrication process. Regarding fabrication of half cells, we planed to use hydroforming instead of spinning in order to reduce costs. Regarding annealing, we had

to decrease the temperature so as not to reduce the mechanical strength of the cavities. Furthermore, we wanted to check the effect of hydroperoxide rinsing on suppressing of field emission. We investigated them by using two single-cell cavities.

We started vertical tests of the TRISTAN scc from September of '87. The problems of surface contamination were solved almost at the beginning of the production period. We often achieved an Eaccmax of 10 MV/m without field emission. However, we again encountered the problem of surface contamination during production. We thus modified the surface-treatment process. Although eight cavities were retreated because of material defects or the input coupler leak problems, the performance of the TRISTAN scc was very good.

During large-scale production of scc, a very high yield rate is required because of the high cost and the tight machine construction schedule. One thus has to fabricate cavities under strict quality control. For this propose, the niobium material must be of a high purity without any inclusions. Secondly, one has to construct a reliable surface-treatment system and establish a quality control method which is useful to each laboratory. CERN, CEBAF, DESY are presently going to start large projects. Other laboratories are also investigating scc application to accelerators. As a result of this situation, it is necessary to describe the surface treatment R & D at KEK and niobium material for large-scale production. Furthermore, it will be useful for the projects following KEK to understand our experiences in TRISTAN scc production. In this paper, we describe them in some detail. From these descriptions, it should be cleared what problems KEK had encountered and how KEK has reached the present technical level.

2. Some Trials and Errors

Between '84 and '85, we tried to make our fabrication process simple. Furthermore, we applied the results of the EP studies described in next section to cavity fabrication. We encountered many problems at that time. Here, we describe six educational experiences among them, which were important for the later development of a surface-treatment system. From these descriptions, one should understand the following: (1) the reason why we can not eliminate the heat treatment in our fabrication process; (2) one reason why we did not try to use positively the helium processing to five-cell cavities; (3) the necessity to carefully select the materials of surface-treatment system, in

order to prevent surface contamination and to increase the reliability of scc RF performance; (4) the motivation for the development of the HR-EP method, which played an important role in the success of TRISTAN scc.

2-1 Effect of Heavy Electropolishing on SCC RF Performance

In our fabrication method, a heat treatment is given to cavities between a first heavy EP(80~130 μ m, EP-I) and a final EP(5~30 μ m, EP-II). If the annealing effect is small, we can omit it and make the fabrication process simple. Figure 2 clearly shows the effect of annealing. The quality factors(Q_0) of the cavities without annealing were lower by two orders of magnitude. However, they were easily improved by annealing. These results mean that we can not omit the heat treatment from our fabrication process.

Origin of Q_0 Dropping

As shown in Fig.3, sample tests of the annealing show highly much hydrogen gas absorption in a heavy EP(90 μ m). Surface analyses (Auger, ESCA) of the highly electropolished samples also an the oxygen and carbon rich contaminated layer of 100 A on the surface. On the other hand, we have recently found that a little amount of sulfur is left on the cavity inner surface by heavy EP. Strictly speaking, we have not yet determined which of them has more influenced on Q_0 dropping. However, the beneficial effects of our measures against hydrogen gas suggest that hydrogen is most influential on cavity performance.

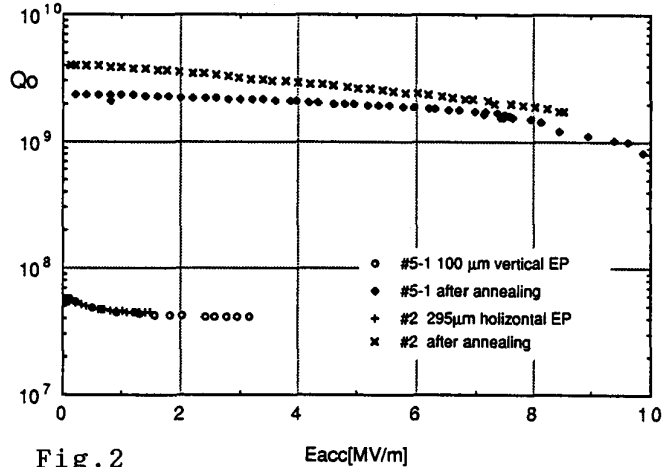


Fig.2 Effect of the heavy electropolishing on scc RF performance.

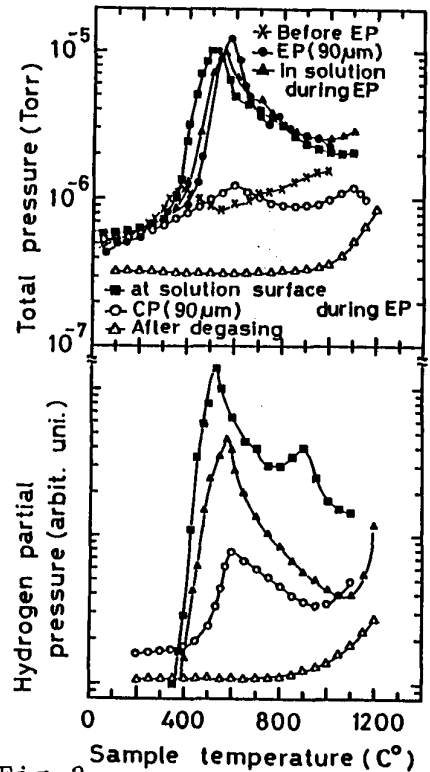


Fig.3 Degassing analyses with highly electropolished niobium samples.

2-2 Sparking Effect

One single-cell cavity achieved an E_{acc} max of 7.6 MV/m. At the end of the measurement, sparking occurred and the quality factor suddenly dropped. After warming up, we measured it again. The quality factor was less than 10^9 and the E_{acc} was limited to 4.8 MV/m by quenching (Fig.4).

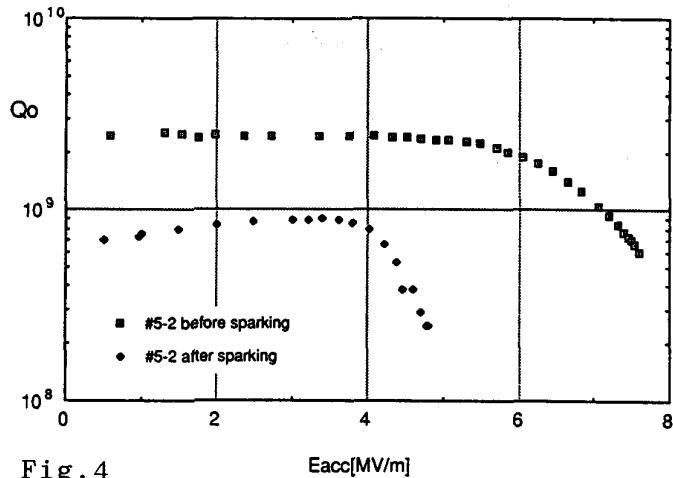


Fig.4
Diference of scc RF performance before and after sparking.

Recovery of SCC RF Performance

After the measurement, we opened the cavity and inspected the inner surface visually. Some sparking marks were found at the straight section near an iris. We ground off the marks and retreated. Then the Q_0 value recovered.

Passivity to Helium Processing

This sparking had no relation with helium processing; since then, however, we worried about sparking during helium processing for multi-cell cavities. This is one reason why we did not passively use helium processing to improve the performance of five-cell cavities.

2-3 Effect with Adhesion of PVC Hose Plasticizer at Alcohol Rinsing

This is one problem with alcohol rinsing during a surface treatment. Fig.5 shows the result in which the plasticizer dissolved to alcohol and adhered to the cavity inner surface. A FTIR (Fourier Transform Infrared Spectroscopy) analysis of the alcohol detected dioctyl phthalate,

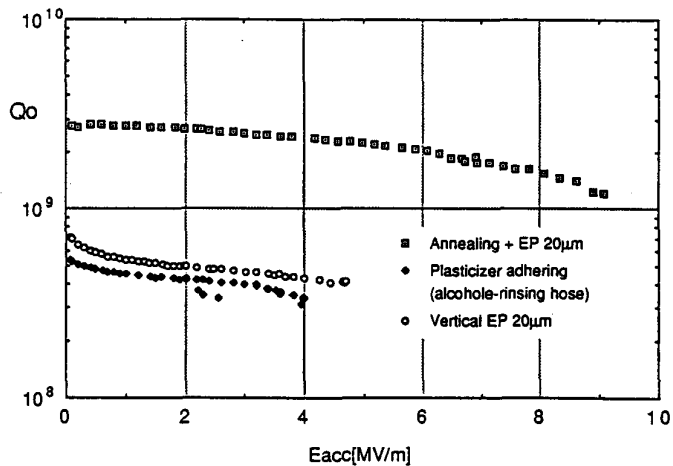


Fig.5
Diference of scc RF performance between PVC hose plasticizer adhesion and its removal.

which was contained within the PVC hose, as a plasticizer. An inorganic substance was also detected which was a stabilizing material of PVC. The degradation in the Q_0 value of one order of magnitude should be due to its dielectric loss.

Recovery of SCC RF Performance

The Q_0 value was not improved by $20\mu\text{ m}$ electropolishing. Though it was improved by annealing($850^\circ\text{C X 1.5 hr}$) and a subsequent, final electropolishing($20\mu\text{ m}$).

Omitting of Alcohol Rinsing

Since then, we have omitted alcohol rinsing from our rinsing process since its effect on scc RF performance was not certain and it only seemed to add additional problems during surface treatment.

2-4 Effect of Adhesion of Plasticizer from Lining Material of EP Solution Tank

Until '85 we used an EP solution tank which was lined with PVC. An EP solution was often stored in it for a long term during studies of the refreshing method of an EP solution (described in next section). During storage, the lining material dissolved into the solution.

Analysis of the EP Solution

We examined the EP solution with an extraction method which is often used in chemical analysis. It is difficult directly analyze since EP solution is highly corrosive. The EP solution was mixed with a carbon tetrachloride (CCl_4) solution. The material dissolved into the EP solution was extracted to CCl_4 . The CCl_4 solution was separated from the EP solution and was analyzed with FTIR and Gas Chromatography. Dihexyl phthalate ($8\mu\text{ g/L}$), dipeptide phthalate($50\mu\text{ g/L}$) and dioctyle phthalate($71\mu\text{ g/L}$) were detected. Since these materials are contained in the plasticizer of PVC, we concluded that they came from the PVC lining material of the EP solution tank.

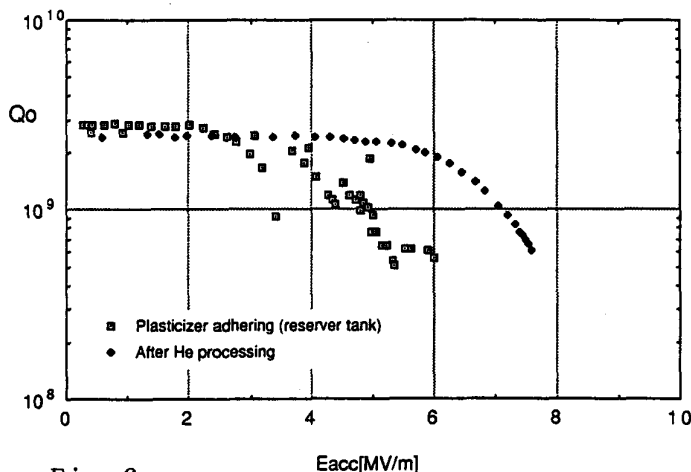


Fig.6 Influence of plasticizer adhesion from solution bath lining material on scc RF performance.

Effect of Plasticizer on SCC RF Performance

Figure 6 shows the RF performance of a cavity which was electropolished with the EP solution mentioned above in the final electropolishing. Heavy field emission which occurred from 3 MV/m could be somewhat overcome by RF processing and helium processing. The Eaccmax reached 7.6 MV/m, though the heavy field emission did not disappear.

From our experience, one can understand that it is necessary to carefully choose the materials for surface-treatment equipment in order to shut out surface contamination by equipment materials and increase up the reliability of scc RF performance.

2-5 Effect of Aluminum Dissolved to EP Solution

Until '85, we used a heat-exchanger made of pure aluminum pipes in the EP solution tank. Since a passive film is generated on aluminum surface, pure aluminum is not corroded by an EP solution consisting of hydrofluoric acid and sulfuric acid. However, it is corroded by either hydrofluoric acid or sulfuric acid. Once we made the mistake of making an EP solution. While thinking that pure aluminum is not corroded by sulfuric acid, we stored sulfuric acid for one night in the tank with the aluminum heat exchanger. The next morning the solution was found to be contaminated with aluminum corrosion. We added hydrofluoric acid to it and made an EP solution contaminated aluminum; we then electropolished a single-cell cavity by 20 μ m.

Effect on SCC RF Performance

Figure 7 shows the result of a cold test of the cavity. Here, Q₀ degradation of two orders of magnitude had no relation with this effect. It was due to heavy electropolishing before this final EP. The noticeable influence of this contaminated EP solution is that field emission started at an Eacc of 1 MV/m. Compared with Fig.2, one can see that field emission occurred at a lower field. One can understand that contaminated EP solution leads to heavy field emission at the lower Eacc.

As presented in the next section, PFA is stable with the EP solution. In order to eliminate corrosion problems by acid, we decided to use PFA instead of aluminum as the heat-exchanger in the new surface-treatment

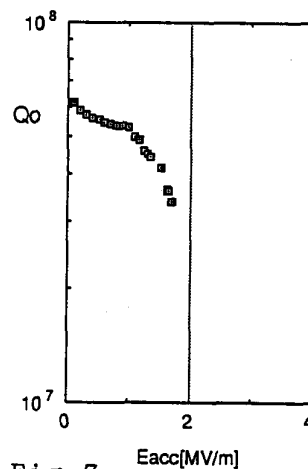


Fig.7 Influence of the aluminum dissolved into an EP solution on scc RF performance.

system for the TRISTAN scc.

2-6 Vertical Electropolishing of Three-Cell Structure

Figure 8 shows the result of vertical electropolishing for the three-cell structure. Q_0 value degradation of several times was observed in the three-cell cavity, compared with each Q_0 value of three single-cell cavities before joining.

Cause of Q_0 Value Degradation

The EP method used for the three-cell cavity during the final EP was a simple application from a single-cell cavity. Figure 9 shows the method for a single-cell cavity ("vertical EP"). We shielded hydrogen gas by a cathode bag made of porous Teflon cloth. Much hydrogen gas is generated in the multi-cell structure.

In the three-cell cavity, hydrogen bubbles which leaked from the cathode bag, grooved the inner cavity surface and made many traces on the surface. The origin of the Q_0 degradation may come from the final electropolishing [3] .

Motivation to Develop a Surface Treatment

This result gave us the motivation to develop an electropolishing method in which hydrogen gas could more easily escape from a multi-cell cavity. As mentioned in next section, the "horizontal rotational EP" method, in which the cavity is electropolished in the horizontal position under rotation, was suitable for this purpose (see Fig.23). Since then, we had made many development efforts.

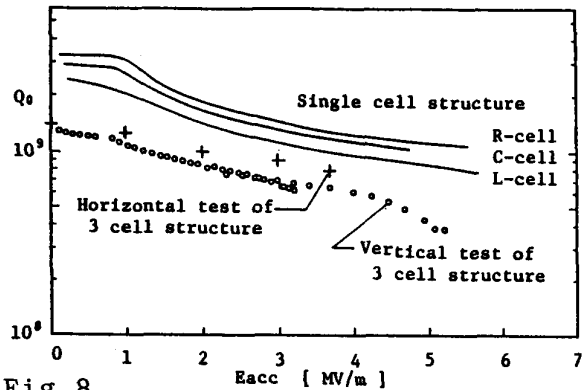


Fig.8 Q_0 -Eacc curves of a three-cell cavity electropolished using the vertical EP method. R,C,L-cell are single cell cavities before completing the three cell cavity.

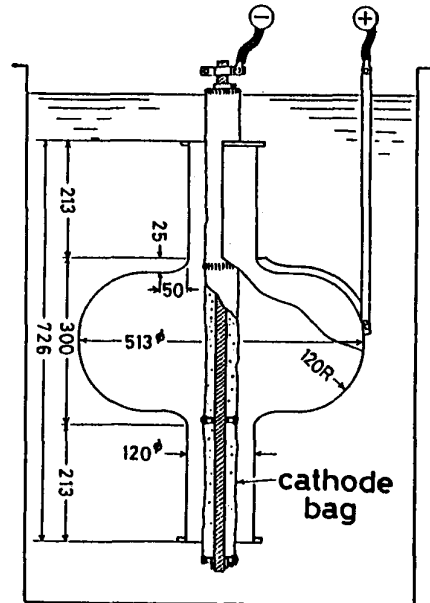


Fig.9 Vertical electropolishing method for single-cell cavities during the final EP.

3. Development of a Surface Treatment System

As presented above, we had to improve the electropolishing for multi-cell structures. In addition, thinking of the TRISTAN scc, we were required to develop a surface-treatment system in which quality control was easy and the hydrogen gas problem could be solved for multi-cell structures. Our concerns in these studies were:

- 1) to search for the most important parameter in niobium electropolishing from the point of quality control,
- 2) to establish a control method of the EP solution,
- 3) to select materials for the surface-treatment system, and
- 4) to develop a horizontal rotational EP method.

Here, we describe in some detail the results of these studies.

3-1 Most Important Parameter in Niobium Electropolishing

Electropolishing has many parameters such as voltage, current density, bath temperature, electrodes configuration, current oscillation and solution concentration, etc. It is well known that current oscillation is important in niobium electropolishing [5] . We had employed the method (current oscillation control) up to 1984. Current oscillation falls away with the current feeding time. To recover it, one has to agitate the solution. One must repeat the alternative process of current feeding and agitation of the solution, in order to continue electropolishing under the current oscillation control method [5] . This intermittent polishing process makes the electropolishing complicate. Furthermore, it is difficult to characterize the current oscillation quantitatively so that current oscillation is unsuitable as a quality control parameter of electropolishing. We investigated other parameters to find the proper quality control parameter. As a result, we have found that both the current density and bath temperature are most important in niobium electropolishing. Since they can easily be controlled, they are proper quality control parameters during electropolishing.

Current Density

Figure 10 shows a result of an electropolished surface at various voltages for a bath temperature of 25°C. It indicates

that one can get a bright, smooth surface at a voltage between 8 and 16 V. Figure 11 shows the same result rewritten in terms of current density. A good surface is obtained at between 30 and 100 mA/cm². In this region, no current oscillation occurred during

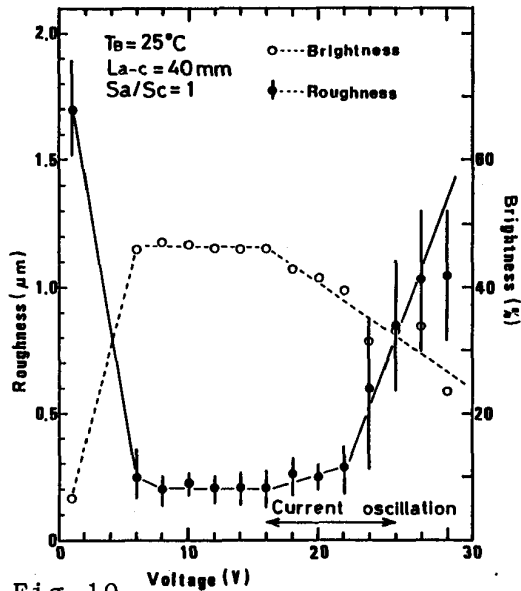


Fig.10 Correlation between voltage and polished states in niobium electropolishing.

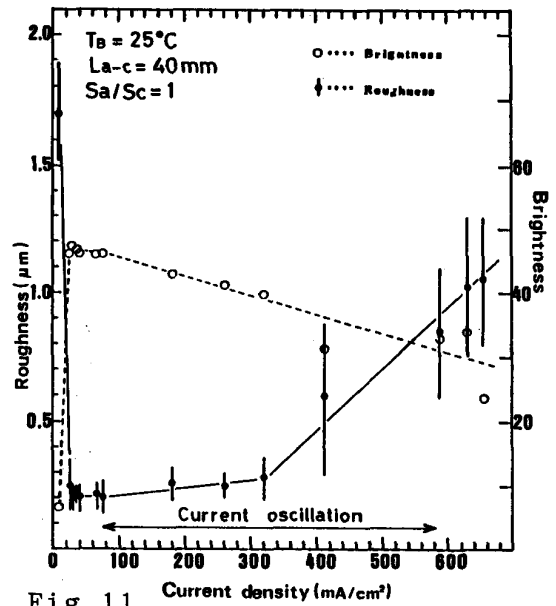


Fig.11 Correlation between current density and polished states in niobium electropolishing.

electropolishing. The current oscillation strongly depends on the electrode configuration.

In this experiment, however, one can not conclude which is more important, the voltage or current density. One can easily vary the current density at the same voltage by the changing the electrode configuration. Figure 12 shows the result of changing the current density from 30 to 320 mA/cm² at 14 and 22 V. The values in the blankets are the current density. In Fig.10, the polished states (roughness and brightness) at 22 V are not so good; Fig.12, however, indicates that at the same voltage one can obtain good surfaces if the current density is decreased to less than 100 mA/cm².

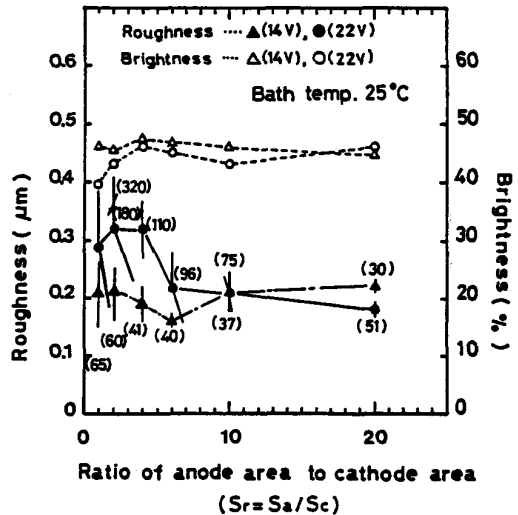


Fig.12 Optimum current density region in niobium electropolishing.

From this result, one can conclude that in niobium electropolishing, the current density is important and its optimum region is between 30 and 100 mA/cm².

Bath Temperature

Figure 13 shows the dependence of the polished state on the bath temperature. The optimum bath temperature range with optimum current density (30~100 mA/cm²) is between 25 and 35°C.

Characteristic Polishing Regions

Furthermore, we have found that there are four characteristic polishing regions, depending on the current density: etching, micro-polishing, macro-polishing and oxygen generation (Figs.14 and 15). In Fig.14, a solid line is a voltage-current density

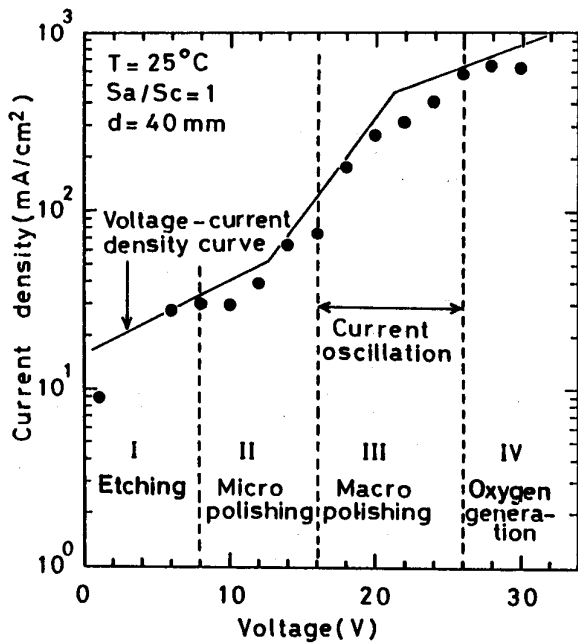


Fig.14 Four characteristic polishing region in niobium electro-polishing.

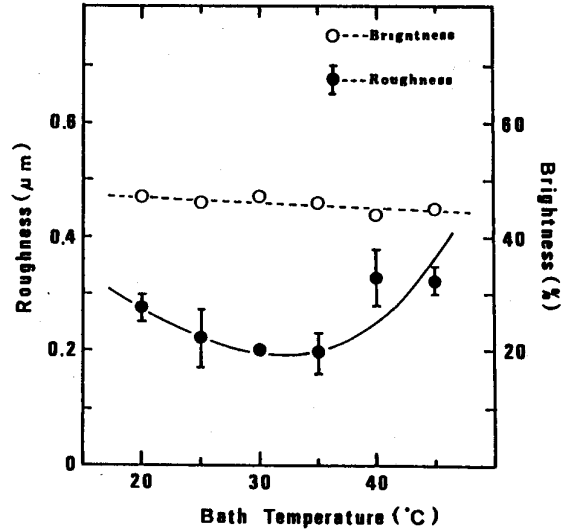


Fig.13 Optimum bath temperature region in niobium electro-polishing.

	Typical roughness	Photograph
I	Etching 25°C, 1V 	
II	Micro polishing 25°C, 10V 	
III	Macro polishing 25°C, 24V 	
IV	Oxygen generation 25°C, 26V 	

Fig.15 Typical polished roughness and photograph of a polished surface.

curve which was obtained by light electropolishing ($5\mu\text{m}$). The black circles are the results of heavy electropolishing ($100\mu\text{m}$). It is fortunate for us that micro-polishing region is in the low-current density range of $30 \sim 100 \text{ mA/cm}^2$, because it is difficult to obtain a large current density in electropolishing of complex structures like multi-cell cavities. This fact caused us to succeed in developing a horizontal rotational EP method (as described later).

3-2 Refreshing Method of EP solution

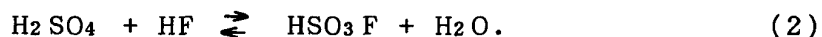
We use an EP solution consisting of 95 ~ 97 % sulfuric acid (H_2SO_4) and 40 % hydrofluoric acid (HF) in the ratio 85 : 10 by volume. For niobium electropolishing, this kind of solution is well known [5] . From the previous situation, estimating the amount of consumed EP solution in the TRISTAN scc large-scale production, it would reach about 300 m^3 . Handling so much solution is very dangerous. The cost of the EP solution is also very expensive. In order to decrease the amount of required EP solution, we developed a refreshing method of the EP solution by adding fluorosulfuric acid (HSO_3F). At the same time, we have found the optimum concentration range of HF in the EP solution. Furthermore, we have established an EP solution control method.

Principle of Refreshing Method of EP Solution

In niobium electropolishing, the following chemical reaction takes place [6] :



From this equation, one can understand that hydrofluoric acid and water are consumed during electropolishing. On the other hand, we have found that the following chemical equilibrium exists in EP solution [7] :



This equation shows the principle of our refreshing method of an EP solution. This means that one can supply HF by adding HSO_3F and water. We can obtain fluorosulfuric acid cheaply on the market.

Experiment of Refreshing Method

Figure 16 is the experimental result of this method using niobium samples. A large amount of niobium was dissolved in an EP

solution by electropolishing (accelerated dissolving). Analyzing, the HF concentration in the EP solution using the fluorine-ion-selective electrode, we calculated the amount of HSO_3F and water to be added, and refreshed the EP solution four times. During the

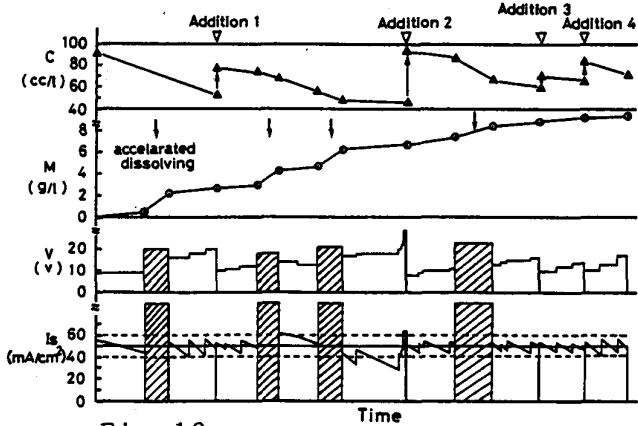


Fig. 16 Sample test on a refreshing method of an EP solution by the addition of HSO_3F .

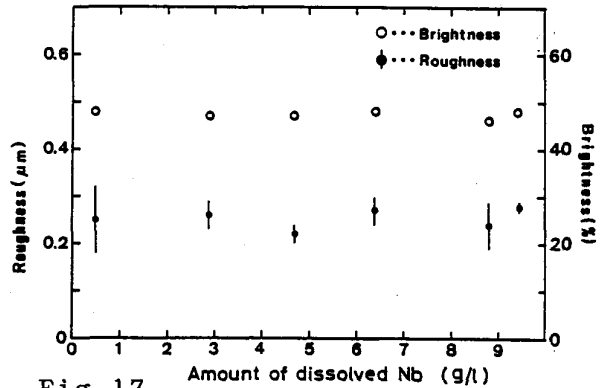


Fig. 17 Polished surface states with a refreshed EP solution.

experiment, we electropolished niobium samples and checked the polished states. Figure 17 shows the polished states by the refreshed EP solution. It can be seen that an EP solution with dissolved niobium of 9 g/L is still usable.

Optimum Concentration of HF

Figure 18 shows the correlation between polished states and the HF (active fluoride) concentration in an EP solution, which is reduced to commercial 46 % hydrofluoric acid. We have found that the optimum HF concentration range is in 60 to 90 cc/L.

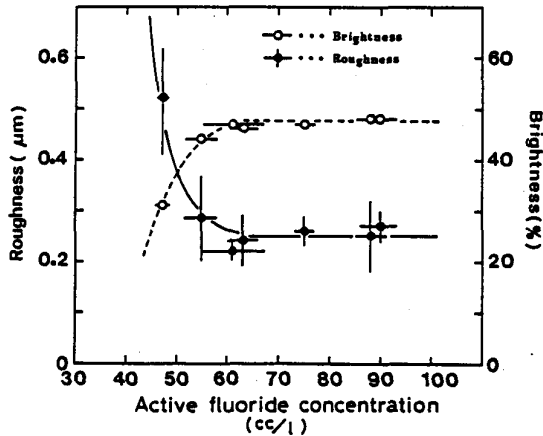


Fig. 18 Optimum concentration of active fluoride (HF) in an EP solution.

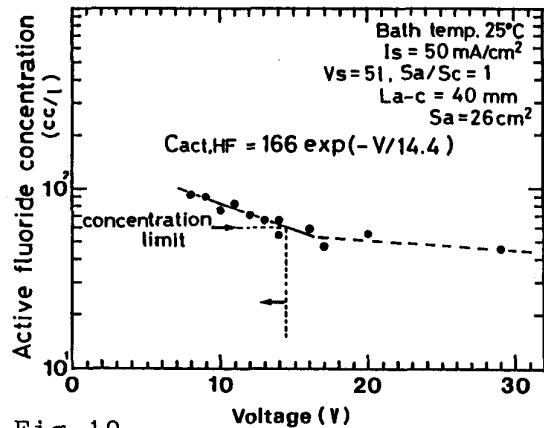


Fig. 19 Relation between the EP voltage and active fluoride (HF) concentration.

Simple Diagnostic Method of EP Solution

In order to examine the HF concentration, it takes about six hours, since it is necessary to use a vaporizing method in the analysis. Instead, there is a simple and speedy method. When the EP solution is exhausted, we have to increase the applied voltage in order to maintain the optimum current density, e.g. 50 mA/cm². Figure 19 shows the relation between the applied voltage and the HF concentration in the EP solution. Electropolishing a niobium sample under the same condition as used in this experiment, if the applied voltage is less than 14 V, one can conclude that the EP solution is optimum. This method is very simple and has a practical importance. We could control the EP solution with this method in TRISTAN scc production.

Application to Cavity Fabrication

Figure 20 shows an application example of this refreshing method to 508-MHz half cells and a single-cell cavity. The EP solution had been stored for five months and refreshed a total of ten times. The last refreshing was carried out for the final EP of a single-cell cavity.

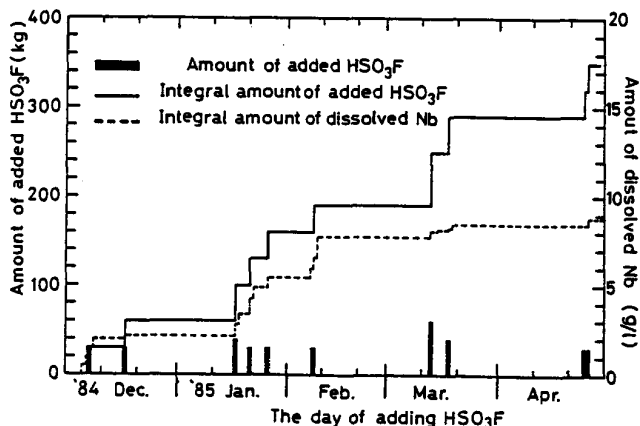


Fig.20 Application of the solution refreshing method to cavity fabrication.

Effect of Refreshed EP Solution on SCC RF Performance

The single-cell cavity was cold tested. The influence of the refreshed EP solution on the scc RF performance was investigated. We could obtain good performance (Eaccmax = 7.6 MV/m, Q₀ = 2.5 X 10⁹ at low field) on the cavity. We confirmed the effectiveness of the refreshing method. At the same time, we established an EP solution control method.

However, long-term storage raised the problem of dissolving the PVC lining material of the EP solution tank. This gave us one motivation to study materials for a surface-treatment system. By this refreshing method of the EP solution, we could reduce the amount of the EP solution required for the TRISTAN scc production from 300 to 10 m³.

3-3 Examination of Materials for an EP System

We investigated what kind of material is most reliable for an EP surface-treatment system. We examined some kinds of plastic materials(PVC, PP, PE, PVDF, PTFE, PFA and Viton) expected to be used for lining materials.

Absorption of an EP Solution

Figure 21 shows the weight change of samples immersed in an EP solution at 40 °C. In Fig.21, the change ratio W is defined as

$$W = 100 \times (w - w_0) / w_0 \quad (\%) \quad (3).$$

Here w_0 is the initial weight and w the weight after immersing in an EP solution. The weight increase is due to absorption of the EP solution by the plastic material or Viton. It indicates that, except for some kinds of Teflon(PTFE, PVDF, PFA), the others exhibit some absorptivity and possibility of swelling. It is better not to use such a material in ball valves, etc..

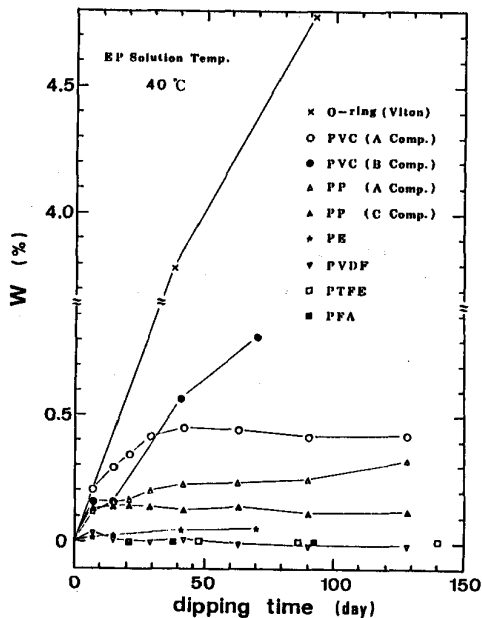


Fig.21
Absorption of an EP solution in various kinds of plastic materials for piping.

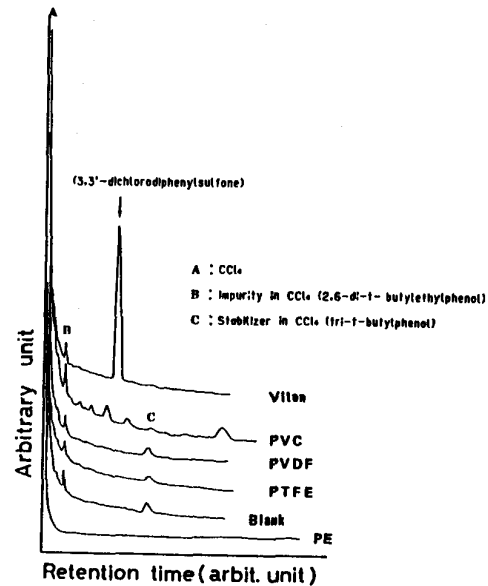


Fig.22
Dissolving of some kinds of plastic materials and Viton into an EP solution for two months dipping.

Dissolving to EP Solution

Figure 22 shows results(Gas Chromatography) regarding the dissolving of materials in an EP solution for two months immersing at room temperature. The analysis method is the same as that mentioned in section 2. In the figure, peak A is CCl_4 . Peaks B

and C represent impurities in the CCl₄ solution, though they are dependent on the purity of the CCl₄ solution used. These impurities are not found in the case of PE, owing to use of the highly pure CCl₄ solution. This result shows that Teflon and PE do not dissolve to an EP solution. Because Viton, which is often used as solution sealing, has some dissolubility to an EP solution, we should be careful of its use.

From the results of these experiments, one can understand that Teflon is most stable in an EP solution and that the second is PE. We decided to use Teflon in the construction of a surface-treatment system for the TRISTAN sec.

3-4 Development of a Horizontal Rotational Electropolishing Method

Horizontal Electropolishing

From a experience concerning the three-cell cavity [3] , we developed an electropolishing method in which hydrogen gas can easily escape through a multi-cell structure. If we electropolish the cavity in the "horizontal" position, the problem seems to be solved. Figure 23 shows applications for a single-cell cavity. The cavity is electropolished by an EP solution half filled. Hydrogen gas escapes from the open mouths at both sides. This "horizontal EP" method was originally presented by H.Diepers and O.Schmidt [8] , a method based on a "current oscillation control" method. Electropolishing is performed in an alternative process of current feeding and agitation of the EP solution: intermittent electropolishing.

Horizontal Rotational Electropolishing

Improving their method based on our original idea, we have developed a new EP system, which was named the "horizontal rotational" EP method (HR-EP), featuring: continuous electropolishing and the closed circulation of EP solution. We employed a "current density control"

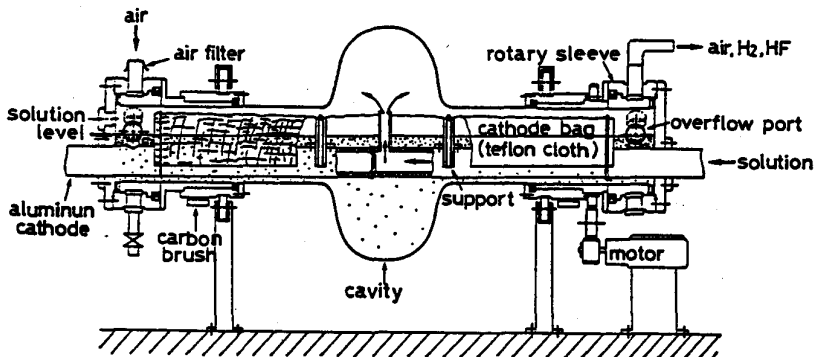


Fig.23
Horizontal rotational EP method for single cell cavities.

method instead of the current oscillation type, making electropolishing very simple.

Idea of Continues Electropolishing

Here, we describe our original idea. As shown before, there is an optimum current density region with niobium electropolishing, suggesting that the thickness of the viscous layer of the niobium complex, generated on the niobium surface by electro-reaction, is important for the leveling mechanism. Continuously rotation of the cavity and circulation of the EP solution give proper agitation to the viscous layer. Suppose that the generation speed of the niobium complex and its dissolving speed by the agitation become the same: the proper layer thickness should be maintained on the niobium surface, so that good polishing can proceed continuously.

Moving Speed of Anode

In order to confirm this idea, first determined a suitable moving speed of an anode using niobium samples. Results are shown in Fig.24. It was found that if the moving speed was less than 10 mm/s, one can obtain a smooth surface by continuous polishing.

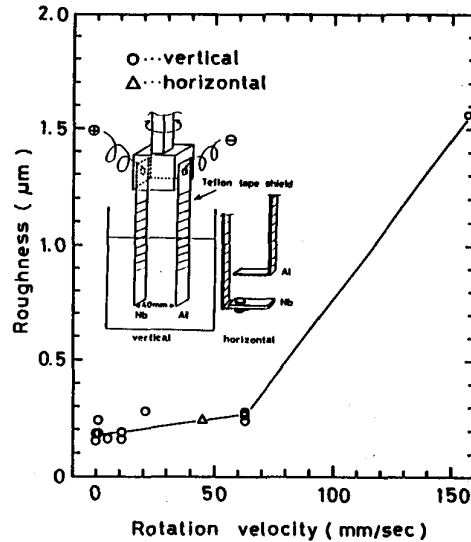


Fig.24 Effect of the moving speed of the anode in an EP solution on polished surface states.

Model Experiments by 1.5-GHz Cavities

We then made half-dividable 1.5-GHz single-cell cavities. We built a HR-EP system for 1.5-GHz single-cell cavities (Fig.25). We searched for the optimum conditions such as cavity rotation speed, solution flow speed and solution temperature. Figure 26 shows a relation between the rotation speed and polished states. Rotation speeds of 1 to 3.5 rpm are good for 1.5-GHz single-cell cavities, and its effect on polished states is small as long as it is

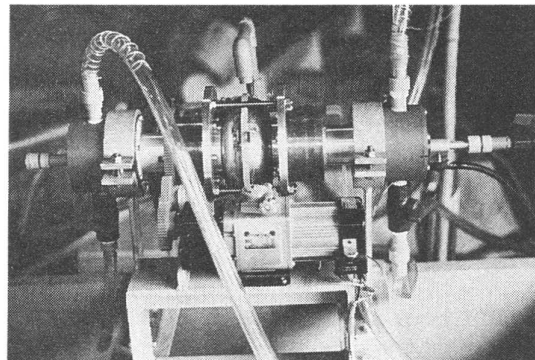


Fig.25 Horizontal rotational EP system for 1.5-GHz dividable single cell cavity.

less than 10 rpm. Figure 27 shows the relation between the flow speed of the solution and the roughness. A slower flow speed is favorable. Figure 28 shows the optimum solution temperature on HR-EP. A temperature between 25 and 35°C is optimum.

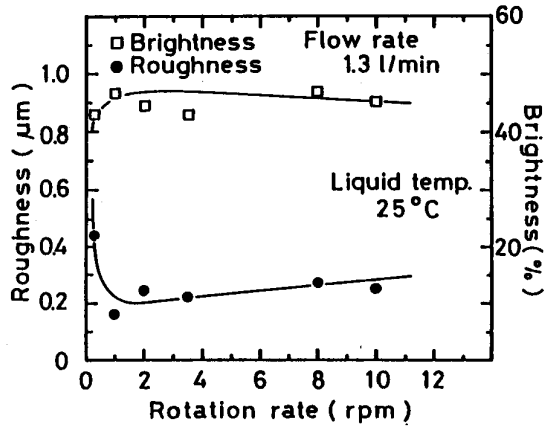


Fig.26 Relation between rotation speed and polished surface state by a 1.5-GHz HR-EP system.

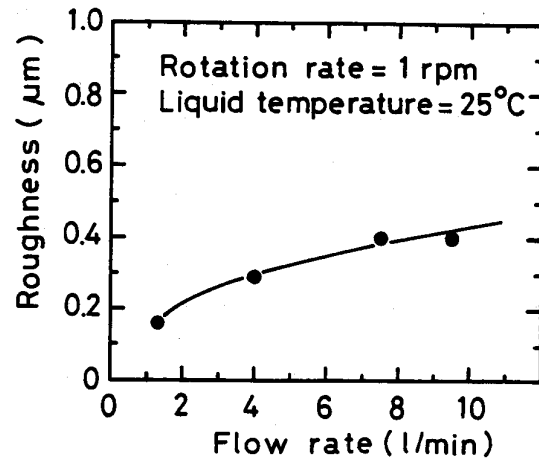


Fig.27 Relation between the flow speed of an EP solution and the polished-surface state.

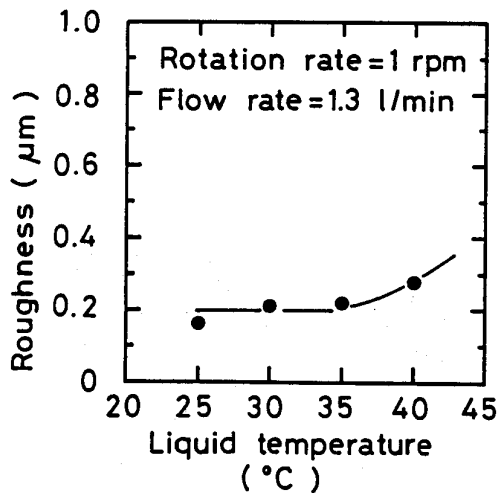


Fig.28 Relation between the solution temperature in the cavity and a polished-surface state.

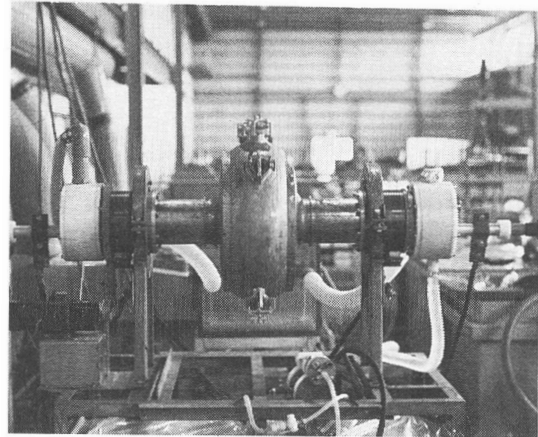


Fig.29 Horizontal rotational EP system for a 508-MHz single-cell cavity.

Scaling to 500-MHz Single-Cell Cavities

In addition, we investigated whether these optimum conditions for 1.5-GHz single-cell cavities were applicable to 500-MHz single-cell cavities, or not. We made a HR-EP system for 500-MHz single-cell cavities (Fig.29). As a result of many studies, we confirmed that the parameters scaled to 500-MHz single-cell

cavities were applicable.

HR-EP System for TRISTAN SCC

We constructed a HR-EP system for the five-cell TRISTAN scc. The system flow chart is shown in Fig.30, a photograph in Fig.31.

The storage tank capacity for an EP solution is 1000 L. It contains a water-cooled heat exchanger made of PFA tubes of 10-mm diameter and 600-meter length. The cooled EP solution is poured through a pure aluminum cathode into the cavity(see Fig.23). The cathode is covered by Teflon cloth(cathode bag) to protect the cavity inner surface from attacking hydrogen gas bubbles. The solution overflowed from the half-level of the cavity returns to the storage tank through the return lines. The EP solution is circulated through a closed system, improving the working environment significantly. There is no smell of hydrogen fluoride. The hydrogen gas generated during EP and some evaporating hydrogen fluoride gas from the solution are exhausted through one of two holes on both rotary sleeves to a scrubber(see Fig.23).

We experienced the fact that lining materials dissolved into EP solution and have bad effects on scc RF performance; we thus used Teflon such as PTFE, PFA and PVD for lining and tubing materials. Teflon packings have also been used for most of the sealing. Viton O-rings were used in some not-replaceable parts. Teflon is very expensive, but it has the highest reliability (Figs.21 and 22).

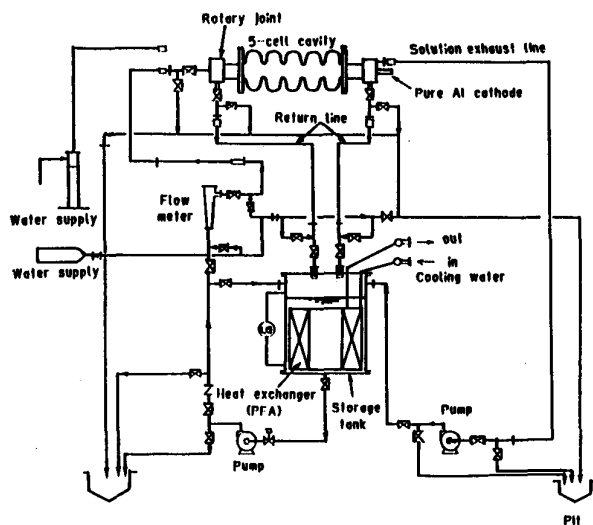


Fig.30
Flow chart of the horizontal rotational EP system for TRISTAN five-cell cavities.

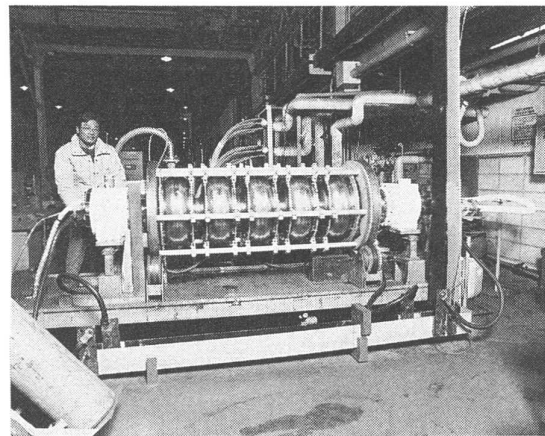


Fig.31
Horizontal rotational EP system for TRISTAN five-cell cavities.

First Use of the HR-EP System for Five-Cell Cavity

The HR-EP system was first used during the final EP(10 μ m) of the AR-#0 cavity, which was the first five-cell cavity we made. However, we obtained a current density of only 25 mA/cm². The cavity inner surface was etched.

The scc RF performance was $Q_0(\text{at low field}) = 3.5 \times 10^9$, the $E_{accmax} = 4.1$ MV/m. E_{accmax} was limited by quenching. In spite of the insufficient EP condition, we could obtain high Q_0 values. The hydrogen problem, which occurred in the three-cell cavity, was thus solved.

4. Development of High Thermal Conductivity Niobium Material

Until now, we have described mostly surface treatment. Here, even though the descriptive flow changes, we describe development of niobium materials, since they have taken important roles for the TRISTAN scc.

Motivation of Development

Understanding niobium materials was also necessary. Fig.1 shows that the third single-cell cavity(fabricated in '82) did not obtain an accelerating field gradient higher than 4 MV/m, in spite of many retreatments. We had suspected niobium material and annealing to be a cause of its low performance. On the other hand, in the 3rd workshop on sc RF of '84, it was shown by H.Padamsee that the higher thermal conductivity of niobium suppresses the thermal instability and increases the achievable accelerating field of sc cavities [4] .

View points of Development

We studied niobium material from two points of view. One is how to limit decreased thermal conductivity of niobium material by absorption of residual gas during annealing. The other is how to increase the thermal conductivity. For the first purpose we employed a titanium wrapping method in annealing. For the second, we succeeded in making highly pure niobium ingots by multi-melting. By combining these technics, we could increase the residual resistive ratio(RRR) of the niobium material from 20~ 40 to 50~ 210, which is proportional to the thermal conductivity at low temperature, as is well known. The achievable accelerating fields of our sc cavities were increased from 6.5 to 11 MV/m.

Here, we describe the effects which the titanium wrapped annealing gives to niobium material and present the development of highly pure niobium ingots. In addition, we discuss the effect of high thermal-conductivity niobium on scc RF performance.

4-1 Annealing with Titanium

As mentioned in section 2, as long as we employ electro-polishing for surface treatment, vacuum annealing of cavities can not be omitted. Since our cavity dimension is large, we must inevitably use an industrial furnace, which has a rather poor vacuum condition ($\sim 10^{-5}$ Torr). Interstitial impurities in niobium material like O, C, N and H reduce the thermal conductivity at around liquid helium temperature [4]. It is therefore important for us not only to develop high thermal conductivity niobium, but also to protect the niobium material from decreasing it by absorption of the residual gas during annealing.

Diffusion of Residual Gas

Figure 32 shows the hardness as a function of the distance from the surface of niobium samples, treated in a poor vacuum furnace (10^{-4} Torr) for a short time (1 hour). The hardness increased with the concentration of interstitial impurities in the niobium material. Such residual gases such as H_2 , O_2 , N_2 and CO can be absorbed as interstitial impurities by niobium during annealing. The figure indicates the diffusion of the residual gas during annealing to the niobium matrix. This figure shows that above 800 °C, diffusion occurs increasingly.

Effect of Titanium Wrapped Annealing

On the other hand, if we wrap niobium samples with a titanium foil and anneal it, we can protect the diffusion. Figure 33 shows the titanium wrapping effect on long-time (5 hours) annealing. In bare annealing, the Vickers hardness of niobium goes up to 130 on the average due to the diffusion of residual gas. However, it

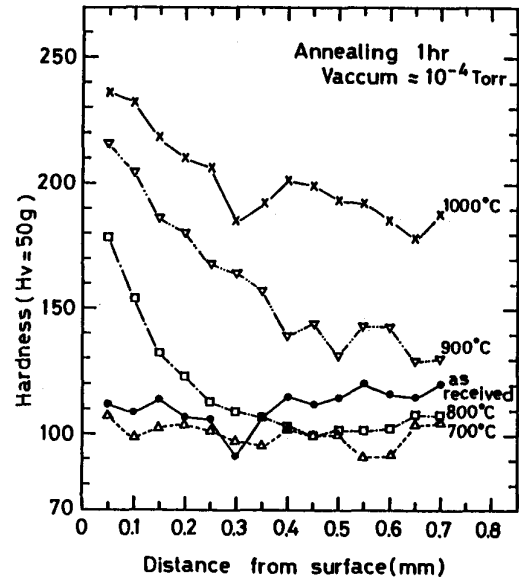


Fig. 32 Absorption of residual gas by niobium under poor annealing vacuum conditions.

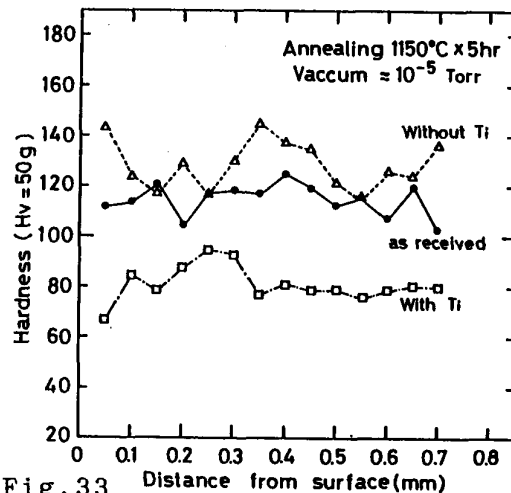


Fig. 33 Titanium wrapping effect against absorption of residual gas during annealing.

decreases to 80 in the case of titanium wrapped annealing.

In addition to hardness measurements, we analyzed the amount of oxygen gas in niobium samples which were annealed both with and without titanium. In bare annealing, it increased to 130 ppm from 80 ppm at 1050 °C X 3 hrs. In the case of titanium wrapped annealing under the same conditions, it was 80 ppm and did not change before annealing. We confirmed the effectiveness of annealing with titanium at around 1000 °C.

RRR Measurement

We started measuring the RRR of niobium material instead of directly measuring the thermal conductivity, which was rather troublesome. RRR can be readily measured using the four-points method. In our measurement, it is defined as follows:

$$RRR = \rho (293.15 \text{ K}) / \rho (9.3 \text{ K}) \quad (4).$$

Effect of Rolling on Gas Absorption of Niobium

Figure 34 shows the effect of rolling and titanium wrapping on niobium gas absorption. At an annealing temperature of 1050°C, the RRR of unrolled niobium material dropped from 74 to 63 after 3 hours of bare annealing. The RRR of rolled(20 %) niobium material dropped to 64. It dropped further to 31 upon the subsequent 2 hours bare annealing at 1050°C.

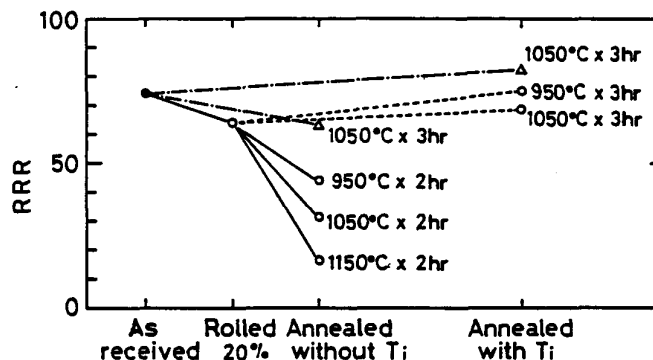


Fig.34 Effect of rolling and Ti wrapping on absorption of residual gas during annealing.

From this result, one can understand that such processes as rolling make niobium more active and niobium easily absorbs the residual gas. This indicates that one should be careful about material or cavity annealing, in such a case niobium is worked by rolling, spinning or hydroforming.

However, using the titanium wrapping method, it can be protected. In Fig.34, comparing the results with and without titanium at 1050 °C, one can easily understand this fact.

Effect of Rolling on Niobium Mechanical Properties

Figure 35 shows the effect of rolling on RRR and the mechanical properties of niobium. Here, we define the rolling

ratio(R) as follows:

$$R = 100 \times (t_0 - t) / t_0 \quad (\%). \quad (5)$$

Here, t_0 is the thickness of the niobium sheet material before rolling and t is that of after. Since the RRR decreases slightly with the rolling ratio, we do not need to worry very much about RRR dropping in the cavity forming process. On the other hand, it has strong effects on the elongation and yield strength.

RRR Change in Cavity Fabrication Process

In Table 1, we show the RRR change during each step of the cavity fabrication process, even though this process is an old version. A new fabrication process is given in Table 2 for the TRISTAN scc. When we start from ingots with $RRR = 75$, as long as we anneal niobium sheet material and the cavity with titanium, we can finally obtain a cavity with $RRR = 100$.

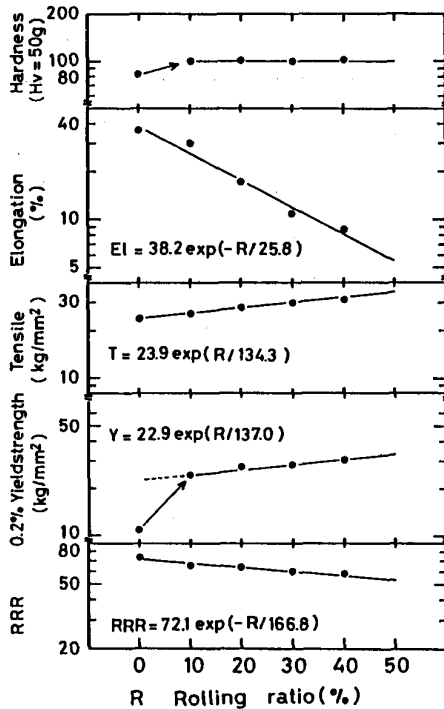


Fig.35
Effect of rolling on niobium mechanical properties.

Tab.1
Change of RRR in each cavity fabrication process.

Proc. No.	Process	RRR	Comment
1	Ingot	75 ± 11	4th melting
2	Forging	75 ± 9	730°C hot forging
3	Rolling	60 ± 8	
4	Material annealing	91 ± 11	850°C, 1.5hr with Ti
5	Spinning	80	
6	Electropolishing (parts)	75	vertical EP 100 μm
7	Electron beam welding	75	EBW seam rrr not change
8	Cavity annealing	100	850°C, 1.5hr with Ti
9	Final electropolishing	100	vertical EP 20 μm

4-2 High thermal conductivity niobium material

As presented above, if titanium wrapped annealing is used, RRR does not decrease in the cavity fabrication process. Then, the problem of highly thermal conductivity niobium is attributed

to making highly pure niobium ingots. We thus concentrated on how to make highly pure niobium ingots. Regarding the improvement of niobium ingots, the following terms are important [4] :

- a) Increasing the number of melting ingots
- b) Improving the vacuum pressure of the melting chamber
- c) Increasing the temperature at the melting zone
- d) Slow melting of ingots.

Effect of Multi-Melting

In these terms, a) can be easily achieved without changing the electron beam melting system. Figure 36 shows the effect of multi-melting on RRR. One can see that ingots with RRR = 80~100 can be made by melting 4~5 times. The vacuum pressure of the industrial EBW system used saturated at 10^{-4} Torr after the third melting. It was thus thought to be meaningless to increase the melting number more than 5 times. We therefore chose a melting number 4-times that of the niobium materials for the TRISTAN scc.

Improvement of EBM System

Under large-scale production of niobium material for the TRISTAN scc, in addition to multi-melting, we applied slow melting and introduced a natural cooling method after the final melting. During the course of production, the maker changed the melting system to the new one from Leybold Heraus.

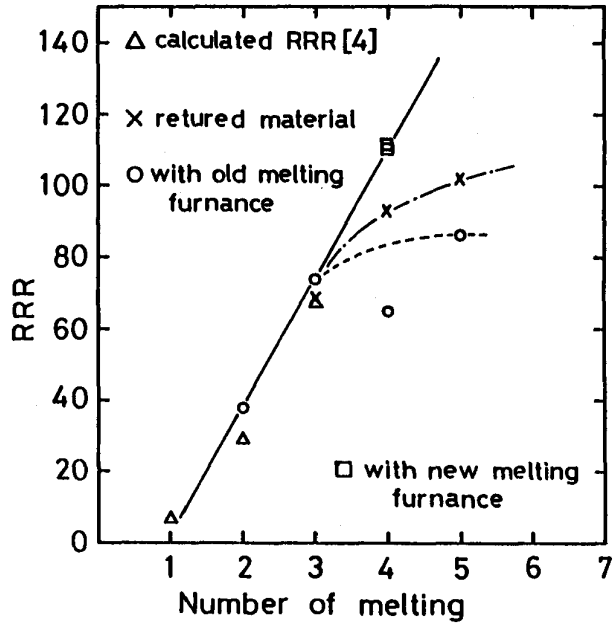


Fig.36 Effect of multi-melting of niobium ingots on RRR.

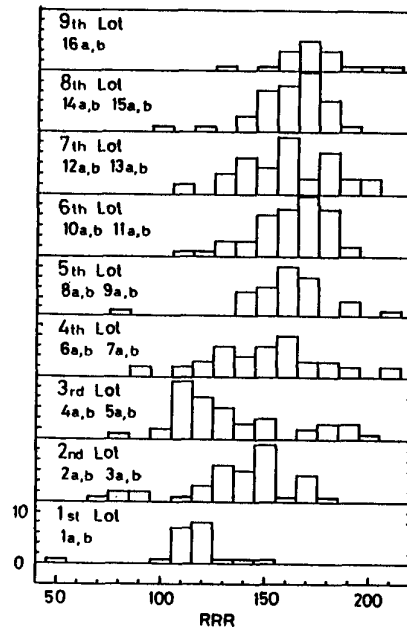


Fig.37 RRR distribution of niobium sheet materials for TRISTAN scc.

Using this new system, the vacuum condition is greatly improved and the melting power increased. As shown in Fig.36, we finally could increase RRR of the ingots to 110 using the new system.

RRR of Niobium Material of TRISTAN SCC

Figure 37 shows the variation of the RRR values of sheet materials for the TRISTAN scc. These niobium sheet materials were annealed in a titanium box at 700 ~ 900 °C for 2 hours. By using titanium wrapped annealing and making highly pure niobium ingots, we could increase RRR from 20~ 40 to 50~ 210 in the TRISTAN scc.

4-3 Effects of High Thermal Conductivity Niobium Materials

The effects of a high thermal conductivity niobium material on scc RF performance are summarized in two terms.

Effect on Achievable Accelerating Field Gradient

One is concerned with the achievable maximum field gradients. A model calculation has shown that the quenching field caused by normal conducting defects increases with the square root of the thermal conductivity(κ) [9] ; it thus increases with the square root of RRR.

$$E_{accmax} \propto \kappa^{1/2} \propto RRR^{1/2} \quad (6)$$

Figure 38 shows the correlation between the maximum field gradient and RRR for our 500-MHz single-cell cavities. Roughly speaking regarding the best results, as a result of the RRR increasing from 20~ 40 to 120 , E_{accmax} increased from 6.5 to 11 MV/m, agreeing well with the above estimation (6). In addition, in the first cold test of single-cell cavities, we obtained an E_{accmax} higher than 7 MV/m with a high possibility.

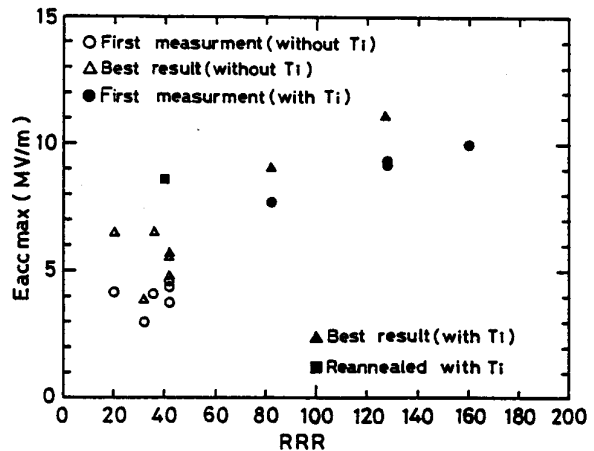


Fig.38 Correlation between RRR and achievable maximum field gradients for 500-MHz single-cell cavities.

Qo-Dropping with Accelerating Field

The other effect of the high thermal conductivity is related to the slope of the Q_0 values dropping with an accelerating field gradient, a phenomenon that must be distinguished from field

emission. This Q_0 dropping can be explained as follows:

" at first the surface temperature increases due to the electro magnetic field on the cavity inner surface, because of surface resistance. The temperature rise then increases the BCS surface resistance according to its temperature dependence in eq.(9), so that at higher field gradients, the surface resistance increases according to an exponential function."

Formulation of Q_0 -Dropping

Here, we represent the "slope" by such cavity parameters as the thermal conductivity, wall thickness, geometrical factor and so on. The surface resistance (R_s) and BCS surface resistance (R_{BCS}) of the sc cavity are given in eqs. (7) and (9), respectively:

$$R_s = \Gamma / Q_0 , \tag{7}$$

and
$$= R_{BCS}(T) + R_{res} , \tag{8}$$

$$R_{BCS} = A \cdot (f^2/T) \cdot \exp(-\Delta / k_B T) . \tag{9}$$

Here, Γ is the geometrical factor of the cavity, R_{res} is the residual surface resistance which has no temperature dependence, f is the RF frequency and 2Δ is the superconducting energy gap. On the other hand, the equation of thermal conductivity and other equations by cavity geometry are given as

$$P_{loss} / S = \kappa \cdot (T - T_B) / d , \tag{10}$$

$$E_{acc} = Z \cdot [P_{loss} \cdot Q_0]^{1/2} , \tag{11}$$

and

$$E_{sp} = a_{sp} \cdot E_{acc} . \tag{12}$$

Here, P_{loss} is the total loss on the cavity wall, S the effective heating area, T_B the bath temperature and d the wall thickness. E_{sp} is the surface peak field gradient. A change of Q_0^{-1} , which is generated by the surface temperature increase, is given by the differential of eq.(7),

$$\Delta Q_0^{-1} = \Gamma^{-1} \cdot \frac{\partial}{\partial T} R_s \cdot \Delta T . \tag{13}$$

The surface-temperature increase is obtained by differentiating eq.(10) and rewriting it as a function of E_{acc}^2 , using eq.(11),

$$\Delta T = (d/S \cdot \kappa) \cdot \Delta P_{loss} \\ = (d/S \cdot \kappa) \cdot [-E_{acc}^2 / (Z^2 \cdot Q_0^2) + 1 / (Z^2 \cdot Q_0)] \cdot \Delta E_{acc}^2. \quad (14)$$

In the case of a sc cavity, Q_0 is very high. Upon eliminating the first term in eq.(14), we can obtain a differential equation for the exponential function on Q_0^{-1} . Using eq.(12), rewriting E_{acc}^2 by E_{SP}^2 , the solution is

$$Q_0^{-1}(E_{SP}^2) = Q_0^{-1}(0) \cdot \exp(\alpha \cdot E_{SP}^2) \quad (15)$$

or $Q_0(E_{SP}^2) = Q_0(0) \cdot \exp(-\alpha E_{SP}^2)$, where $(15')$

$$\alpha = R_s(T) \cdot d \cdot (\Delta / k_B \cdot T - 1) / (T \cdot \kappa \cdot S \cdot Z^2 \cdot \Gamma \cdot a_{SP}^2) \text{ and } T = T_B. \quad (16)$$

If α is small, well-known E_{SP}^2 dependence of inverse Q_0 is obtained.

$$Q_0^{-1}(E_{SP}^2) = Q_0^{-1}(0) \cdot (1 + \alpha \cdot E_{SP}^2). \quad (17)$$

Figure 37 shows the Q_0 - E_{SP}^2 curves for a single-cell cavity and a TRISTAN five-cell cavity. They are well fitted by an exponential function.

Effect on Q_0 -Dropping

Eqs.(15') and (16) show other merits of high thermal conductivity against the Q_0 value dropping with the accelerating field increasing. If the other parameters, except for the thermal conductivity, are the same, Q_0 dropping slope(α) becomes small in proportion to the thermal conductivity. This means that one can maintain high Q_0 values at high fields by the use of high thermal conductivity niobium (Fig.39).

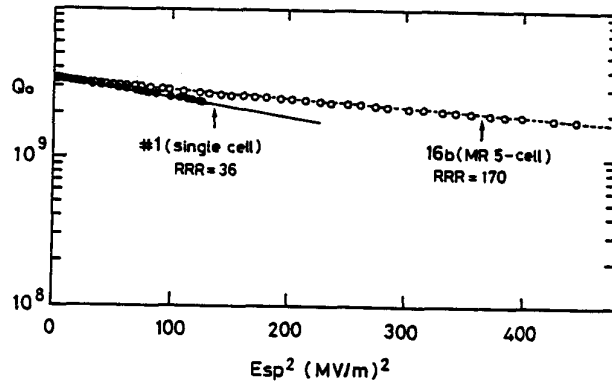


Fig.39 Q_0 - E_{SP}^2 curves for single and five cell cavities which have different RRR.

5. Complete Application of HR-EP for Five-cell Cavities

Here, we again describe the surface treatment. As mentioned in section 3, we developed the HR-EP system during the end of

'85. The hydrogen gas problem encountered in the three-cell cavity was solved by using this system. However, it had the problem to obtain a well electropolished surface. In order to solve this problem, we had to obtain a high current density, at least higher than 30 mA/cm².

5-1 Optimum Condition of HR-EP for Five-Cell Cavities

After performing the beam test by the AR-#0, we investigated why we could obtain only 25 mA/cm² in the first HR-EP application. A problem was found in over-covering by a cathode bag. Furthermore, in searching for optimum HR-EP conditions for a five-cell cavity, the optimum parameters were found to be:

Flow ratio of solution = 60 l/min,
Rotating speed of cavity = 0.4 ~ 1.2 rpm,
Solution temperature in the cavity = 25 ~ 35 °C,
Average current density = 50 ~ 60 mA/cm².

5-2 Use of HR-EP for Heavy EP of Five-Cell Cavities

Between '86 to '87, we fabricated two five-cell cavities (AR-#1,2) to start scc operation in AR. This term, we were preparing for TRISTAN scc production. In order to make electropolishing simple, we had to do the following:

- 1) Confirm the feasibility of complete application (EP-I and EP-II) of HR-EP for five-cell structures.
- 2) Check what kind of problems occur; whether to employ a used EP solution at EP-II to reduce the amount of EP solution.

Our concerns were considered in the fabrication of AR-#1,2. Figure 40 shows EP-I data by HR-EP such as current, voltage, EP solution temperature in the reservoir and EP solution temperature in cavity. The polishing speed was 0.4 μ m/min. Figure 41 shows the removed thickness distribution and the current density distribution in EP-I. The average removed thickness was 80 μ m. The current density distribution was calculated from the removed thickness. An average current density of 52 mA/cm² was obtained. In the equator parts where it is difficult to obtain a sufficient current density, a current density of 40 mA/cm² was obtained. The current density was in the optimum range in all areas, except for beam pipes. Thus all inner surfaces were electropolished like a mirror. We could confirm that HR-EP had no problem regarding heavy electropolishing.

Trial to Employ the Used EP Solution in EP-II

We wanted to decrease the amount of EP solution, because of cost reduction. After EP-I, the AR-#1 cavity was electropolished by $6\mu\text{m}$ (EP-II), using EP solution in which 1.7-g/L niobium was

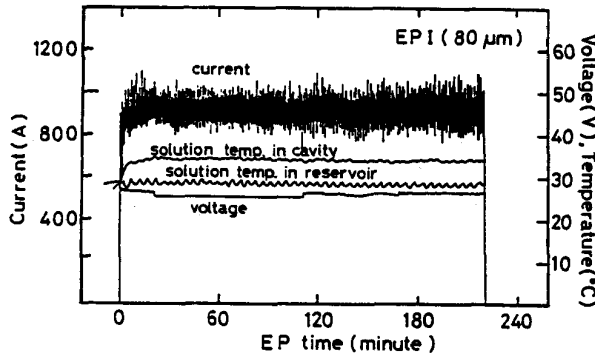


Fig. 40
Data records of a horizontal rotational EP of the TRISTAN scc for EP-I ($80\mu\text{m}$).

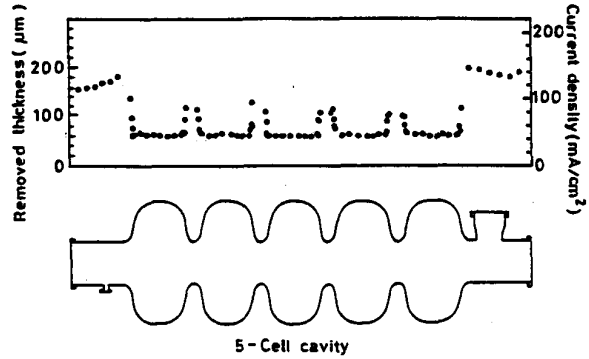


Fig. 41
Removed thickness distribution for a five-cell cavity by horizontal rotational EP.

dissolved. After EP-I by the same EP solution, the AR-#2 cavity was subsequently electropolished by $5\mu\text{m}$. The amount of dissolve niobium in the EP solution was then 3.7 g/L.

SCC RF Performance

In Figs. 42 and 43, we show the results of a cold test. The Q_0 value of AR-#1 (Fig. 42) suddenly jumped upward at 5.5 MV/m during RF processing. The maximum accelerating field reached 6.4 MV/m. Finally, the Q_0 value at 5 MV/m was 2.5×10^9 . The maximum field was limited by quenching.

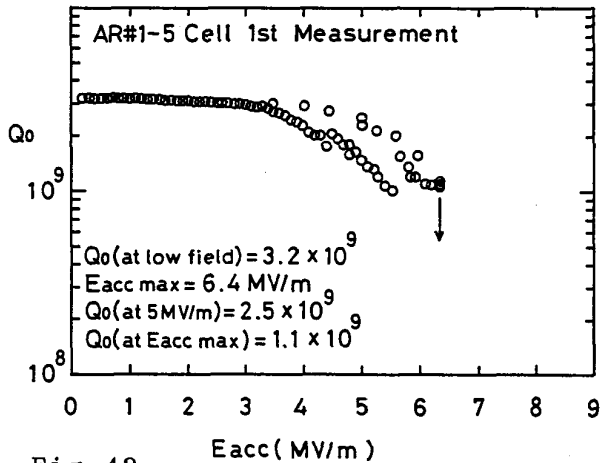


Fig. 42
 Q_0 -Eacc curve of the AR-#1 five-cell cavity during the first cool-down.

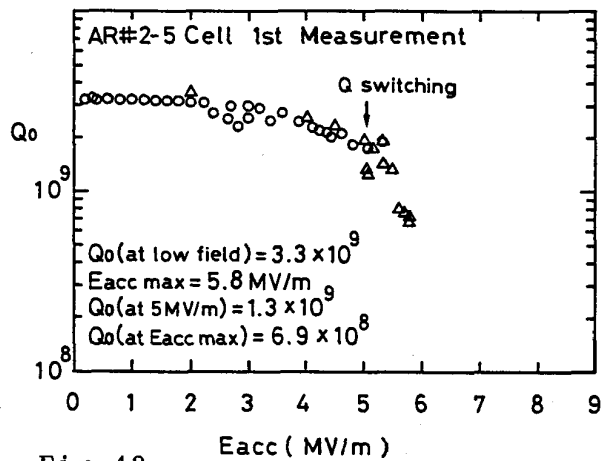


Fig. 43
 Q_0 -Eacc curve of the AR-#2 five-cell cavity during the first cool-down.

The AR-#2 cavity (Fig.43) reached an Eacc of 5.2 MV/m with short RF processing, though the Qo value suddenly dropped from 2.0×10^9 to 1.4×10^9 at the field. There was no improvement in recovery by RF processing(Qo-switching). Heavy field emission occurred from 3.5 MV/m. Finally, the Qo value at 5 MV/m was 1.3×10^9 . The Eaccmax was 5.8 MV/m, limited by the field emission.

Analysis of Niobium Surface

In those EP-II, we set niobium samples in the higher-order mode coupler ports on the equator of one end cell and on the one beam tube, in order to investigate the polished surface states. Figure 44 is the result of surface analysis of the sample with EPM(Electron Probe Microanalyzer). As can be seen in a SEM image, some stains were found on the surface. By element analysis, large particles (200 μ m) were found to consist of aluminum and sulfur. The other small particles (10 μ m) were silicon and iron. We mechanically ground the inner surfaces of all half cells before EP-I. Except for sulfur, these compositions are contained in the buffing abrasive.

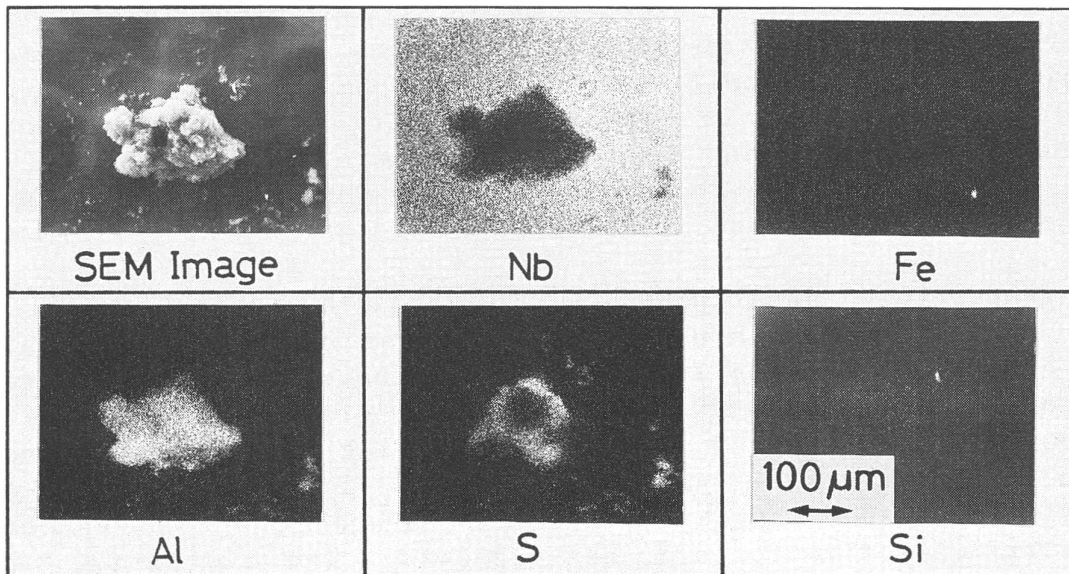


Fig.44
Surface analysis of the substance adhered on niobium sample in HR-EP.

Origin of Qo-Switching or Field Emission

The buffing abrasives, which were left on the surface, came out to the EP solution at EP-I, polluting the EP solution. Since these cavities were finally electropolished with the polluted solution, stains again adhered to the niobium surface. Perhaps

the origin of Qo-switching or field emission was due to these buffing stains. If one were to use a fresh EP solution at EP-II, this problem should be solved. From our trials, it was concluded that one must use fresh solutions in EP-II so as to eliminate Qo-switching or field emission.

6. Some Checks of the TRISTAN SCC Production Process

Before going into large-scale production of the TRISTAN scc, it was necessary to check a few items:

- (1) Effect of hydroforming on scc RF performance.
- (2) Effect of 700 °C annealing on scc RF performance.
- (3) Effect of hydroperoxide rinsing on field emission.

Change of Forming Method

The development of niobium material (described in section 4) increased the workability of niobium material, allowing hydroforming of the half cell of the 508-MHz scc to become possible. Hydroforming is suitable for large-scale production because it is simple and less costly. Therefore, in the TRISTAN scc, it was employed. The aim of (1) is to check if the change in the forming method has some kind of effect on scc RF performance.

Low Temperature Annealing

Highly pure niobium development has caused the mechanical properties of niobium to decrease. We therefore had to decrease the annealing temperature in cavity heat treatments to be as low as possible. Our aim of regarding annealing is to degas hydrogen in niobium matrix which comes during EP-I. As shown in Fig.3, sample tests show that at a low temperature of 700 °C, annealing is still effective for hydrogen degassing. The aim of (2) is to confirm this by using cavities annealed in an industrial furnace.

Effect of Hydroperoxide Rinsing on Field Emission

We often experience the smell of sulfurous compounds when we open cavities after measurement. This smell will be caused by the decomposition of sulfuric acid in EP solution. Sulfur in Fig.44 is one of the decomposition products of the sulfuric acid. In those days, we suspected that decomposition products are causes of field emission. It is well known that one can remove the decomposition products with a hydroperoxide rinsing [10] .

The aim of (3) is to check the hydroperoxide rinsing effect on field emission.

Effect of Hydroperoxide-Rinsed Niobium Surface

Before cavity tests, we studied the surface states of niobium rinsed with hydroperoxide using ESCA and Auger. From those results, we could not obtain a clear conclusion about the hydroperoxide rinsing effect on removing sulfurous compounds. However, the following effects were sought [11] :

- (1) Generally, an electropolished niobium surface has a niobium pentoxide layer ($\sim 10\text{\AA}$), with some unsaturated niobium oxide layers ($\sim 50\text{\AA}$) underneath. Hydroperoxide-rinsing oxidizes unsaturated niobium oxide and changes it to niobium pentoxide. This effect seems to be effective on scc RF performance. Because unsaturated niobium oxides are resistive, but niobium pentoxide is a complete insulator, the RF loss should be reduced.
- (2) Hydroperoxide-rinsing seems to reduce carbon contamination on the niobium surface, and causes us to expect the reduction of the field emission.

Experiments

To check above-mentioned effects, we tested hydroperoxide-rinsing using two single-cell cavities. These cavities were fabricated by hydroforming, using niobium material with a RRR value of 120. After EP-I, they were annealed at $700\text{ }^{\circ}\text{C}$ for 1.5 hours with a titanium box. They were finally electropolished by $5\text{ }\mu\text{m}$. In these electropolishing the EP solution used for AR-#1 and #2 cavities was used again. At the final EP, the hydroperoxide-rinsing (10 % V/V , 20 min) was introduced into one cavity, but not introduced to the other.

SCC RF Performance

Figure 45 shows the result of a cavity without hydroperoxide-rinsing, Figure 46 one with. In both cases, the Q_0 values fluctuated from an accelerating field of 4.5 MV/m due to the use of a polluted solution. Both reached 9 MV/m by RF processing. The hydroperoxide-rinsed cavity showed Q_0 dropping at 5.4 MV/m, similar to that of AR-#1,2, but recovered by RF processing. Its maximum field was limited by the field emission and its Q_0 -Eacc curve was stabilized by helium processing. The Q_0 value at 5 MV/m was, finally, 2.6×10^9 .

The cavity without hydroperoxide-rinsing also showed Q_0 -switching at 7 MV/m(Fig.45); it did not recover by subsequent RF

processing. Furthermore, during helium processing it had heavy field emission from 6 MV/m and its maximum field was limited to 7.2 MV/m by quenching. Its Q_0 value at 5 MV/m was 1.9×10^9 .

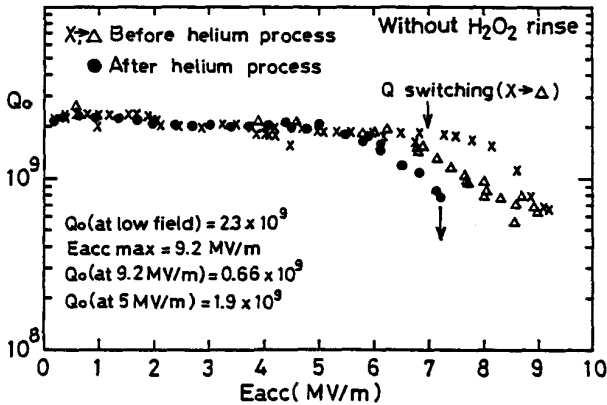


Fig.45
 Q_0 -Eacc curve of a single cell cavity without H_2O_2 rinsing.

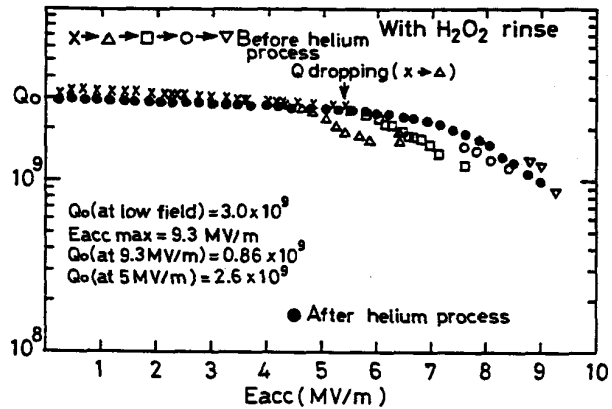


Fig.46
 Q_0 -Eacc curve of a single cell cavity with H_2O_2 rinsing.

Conclusions from Experiments

From these cold tests, one can first conclude that hydroforming and 700 °C annealing have no problem on scc RF performance, but that the use of a polluted solution during final electropolishing makes the Q_0 value fluctuate with an increasing accelerating field. Moreover, it often leads to Q_0 -switching, and is not recovered by RF processing.

As for hydroperoxide-rinsing, two differences were observed phenomenologically. One is the effect on helium processing. The hydroperoxide-rinsed cavity was not changed upon Eacc by helium processing, while the non-hydroperoxide-rinsed cavity quenched at a lower field than that before helium processing. The reason of this phenomenon is obscure. It might be caused by particles included in the helium gas. Another effect concerns the difference in the absolute Q_0 values. One can see significantly the difference in Q_0 values between the two cavities(Figs.45 and 46). The Q_0 value of the hydroperoxide-rinsed cavity is higher than that of the non-hydroperoxide-rinsed cavity. The measurement accuracy in both measurements is the same and the RRR value of these cavities is also the same. It is difficult to search for the other origin, except for the difference in rinsing. This would be due to the oxidation effect of unsaturated niobium by hydroperoxide, as mentioned above. We therefore concluded that hydroperoxide-rinsing seemed to improve the scc RF performance, and decided to employ it in the TRISTAN scc. However, the effect of hydroperoxide-rinsing on the scc RF performance is now under

additional study.

7. TRISTAN SCC Large-Scale Production

The large-scale production of TRISTAN scc started from November, 1986, and vertical tests were finished in May, 1989. This is the first large-scale application of superconducting cavities to a storage ring. We measured all cavities, one by one, in a vertical cryostat (Vertical test) and checked what kind of problems still exist in the industrial production. Here, we describe some problems that we experienced.

7-1 Fabrication Process of TRISTAN SCC

In Table 2(1~ 14), we show the fabrication process of the TRISTAN scc.

Material

Niobium material is 2.35 mm in thickness and 720 mm in diameter for a half cell. As presented in Fig.37, we used niobium material having RRR values between 50 and 210. However, almost all had RRR values higher than 100 and an average value of 152.

Forming

Half cells are formed by a hydroforming method developed by Mitsubishi Heavy Industries at Nagoya. After forming, some half cells which had wrinkles were repaired with a hammer. Wrinkles occurred at the round parts of half cells during forming.

Buffing

Their inner surfaces were checked carefully by human eyes. All inner surfaces were then mechanically ground by 30~ 50 μ m. One of the aims was to grind off deep defects (pits) which can not be removed by EP. The other is to obtain smoother surfaces using EP. Because the initial roughness determines the polished

Tab.2
Fabrication process for the TRISTAN scc.

1. Niobium material, 720 ϕ x 2.35 mm, RRR \geq 100.
2. Hydroforming of half cells.
3. Buffing all inner surface of half cells and Visual inspection.
4. Trimming of half cell.
5. Electron Beam Welding of half cells for single cells, Mechanical grinding of the EBW seams(equators) and Visual inspection.
6. EBW of single cells for five cell structure, Mechanical grinding of the EBW seams(irises) and Visual inspection.
7. Pre-Electropolishing 3~ 4 μ m.
8. Electropolishing 80 μ m (EP-I), and Visual inspection.
9. Heat treatment 700 $^{\circ}$ C x 1.5 hours, with titanium box.
10. Pre-Tuning.
11. Final electropolishing 5~ 10 μ m (EP-II).
12. Assembling in clean room (class 100), Vacuum evacuation, and Baking 110 $^{\circ}$ C x 10 hours.
13. Mounting to vertical test stand.
14. Vertical test.
15. Assembling to horizontal cryostat.
16. Horizontal test.
17. Installation to MR tunnel.

roughness by EP, it is important for the initial roughness to be as small as possible, in order to obtain a smooth surface. After grinding, they are degreased and immersed in hydrochloric acid (HCl 18%) for 3 hours in order to remove rust spots on the outside surface. Rusty materials are included at the scars caused by the die. Finally, they are immersed in water for 6 hours in order to check if rust still exists. All inner surfaces are again carefully checked by human eyes.

Trimming and Electron Beam Welding

Half cells are trimmed, one by one, on a lathe by cutting the equatorial part and iris section. They are degreased with trichlorethylene, and then welded at the equator with a defocused electron beam from the outside. Electron beam welding (EBW) seams are mechanically ground and visually inspected. Furthermore, single cells are electron-beam welded at irises, and five-cell structures are built. Again the EBW seams at irises are mechanically ground and carefully inspected with a mirror and telescope.

Pre-EP and EP-I

After degreasing, the EP solution is stored in a five-cell

Tab.3 EP condition.

EP Condition	Pre-EP	EP-I	EP-II
EP Time (minutes)	3 x(2 cycle)	210	13~ 25
Removed Thickness (μ m)	3~ 4	80	5~ 10
Current Density (mA/cm ²)	40	52	52
Currents (A)	600 → 1000	940	940
Voltage (V)	27	25~ 27	27
Temperature of EP Solution in Cavity (°C)	25 → 35	33	33
Temperature of EP Solution in Storage Tank (°C)	-	27~ 28	28~ 29
Rotation Speed (rpm)	1.6	0.7	1.0
EP Solution (l)	130 stored in cavity	1000 refreshed	1000 fresh
Rinsing	1st rinsing 2nd rinsing	1st rinsing 2nd rinsing	1st rinsing 2nd rinsing H ₂ O ₂ rinsing 3rd rinsing Ultra-pure Water rinsing

structure; electropolishing is done at $3\sim 4\mu\text{ m}$ in order to remove buffing abrasive left on the surface(Pre-EP). The solution is dumped. The cavity is rinsed with water. Pre-EP was introduced during coarse of large-scale production (as described in section 7-4). After Pre-EP, the cavity was subsequently electropolished ($80\mu\text{ m}$ on average(EP-I)). The parameters with EP-I are given in Tab.3. The water rinsing after EP-I was stopped by the second rinse(see 7-3). The cavity is then dried in a clean room. The inner surface is inspected visually with a mirror and telescope.

Annealing

Five-cell cavities are annealed in a vacuum at a pressure of 10^{-5} Torr at 700°C for 1.5 hours. Two five-cell cavities are treated once in a titanium box.

Pre-tuning and EP-II

After Pre-tuning [12] , they are again electropolished by $5\sim 10\mu\text{ m}$ (EP-II). Here, we use a fresh EP solution in order to avoid surface contamination by buffing stains and sulfur (as described in section 6). Four five-cell cavities are treated consecutively. Since the amount of removed thickness is little, it is still fresh for four times EP-II. The parameters with EP-II are given in Tab.3. Water rinsing is carefully carried out for a long time. We found it very important to suppress field emission. Our rinsing method is described in detail in section 7-3. After the final ultra-pure water rinsing, the cavity is filled with nitrogen gas and transported to KEK from the company.

Clean Room Assembly

As shown in Fig.47, in a clean room(class 100), the shower pipe is extracted from the cavity which is set at the third rinsing; it is then assembled for vacuum evacuation.

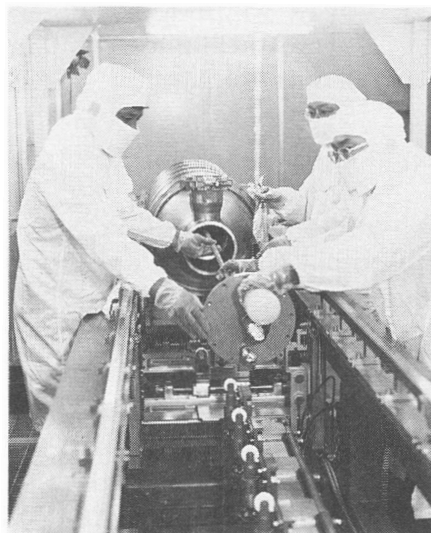


Fig.47
Working in a new clean room (class 100) at KEK.

Evacuation and Vertical Test

Inner surface of the cavity is wet. So we evacuate it with a 260 L/min rotary pump and a 50 L/sec turbo molecular pump while warming up at 60°C . It takes two hours to reach a vacuum pressure of 10^{-6} Torr. After a leak test, it is baked at 110°C for ten hours. After baking, it is evacuated with an ion pump at 160 L/sec. The vacuum pressure reaches 10^{-9} Torr

at the pump head eight hours after baking. It is mounted in a vertical cryostat and measured with 1500 L of liquid helium.

7-2 Measures against Qo-Switching and Field Emission

Use of Fresh EP Solution in EP-II

As a final measure against Qo-switching and field emission, we decided to use a fresh solution at EP-II. In order to carry it out we introduced the "batch mode". As for EP-I, four cavities are subsequently electropolished as one batch, with the same solution being refreshed by HSO₃F. We then disposed the EP solution and changed to a fresh one. We performed EP-II for four cavities in a row. The EP solution is used in the next EP-I. By this mode, the amount of solution for thirty-two cavities was 8 m³.

Reinforcing of Rinsing

In addition, we reinforced the rinsing method after EP-II: the use of hydroperoxide-rinsing and elongation of the rinsing time. The total rinsing time became 1.5 ~ 2 times longer in comparison with those of AR-#1,2. Our rinsing method is described in detail in 7-3.

Assembly in New Clean Room

In addition to these changes, a new large clean room(Class 100) was built at KEK for the assembly of sc cavities(Fig.47).

Overcoming of Qo-Switching and Field Emission

In Fig.48 we show the Qo-Eacc curves of the first two cavities (1a,1b) of the TRISTAN scc. Comparing these results with those of AR#1,2, one can easily see that Qo-switching and field emission problems were solved. These results were obtained by short RF

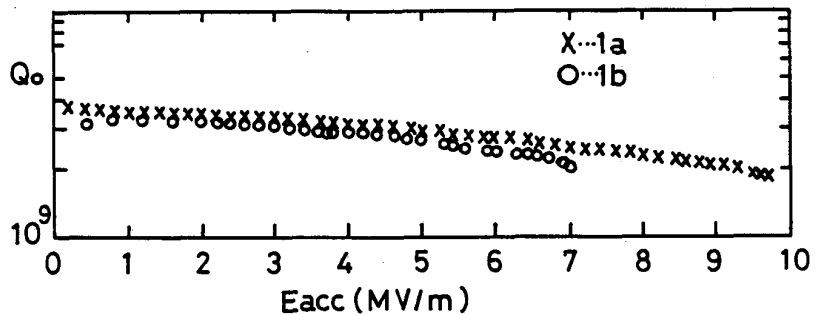


Fig.48
Qo-Eacc curves of the first two five-cell cavities for TRISTAN scc in the vertical measurements.

processing of about one hour. In the case of the 1a cavity, it took two hours to achieve a maximum accelerating field of 9.7 MV/m.

7-3 Rinsing Method

Chemical residue can be a cause of field emission. After we overcame the Qo-switching problem, it became the final problem in our surface treatment. We found that rinsing is important to decrease field emission. This was also confirmed at CERN [13]. We now describe our rinsing method in some detail.

First Rinsing

After the final electropolishing, the cavity is rotated to a vertical position and the EP solution is taken out. Subsequently, demineralized water is poured into the cavity through the cathode pipe. Overflowing and dumping is repeated six times until the PH value of the overflowing water becomes higher than 3. It takes twenty-five minutes from the first pouring to the final dumping.

Second Rinsing

After the first rinsing, we remove the cathode from the cavity, as shown in Fig.49. Moreover, the cavity is laid down and the rotary sleeves at the both beam pipes are taken off. Then, the cavity is raised and transferred to the shower rinsing. The shower rinsing is performed in a vertical position, suspended by a crane, until the PH value of the exhausted water becomes higher than 5. It takes half an hour. The pressure of the shower is less than 5 kg/cm².

Hydroperoxide Rinsing

Subsequently, the cavity is filled with hydroperoxide (semi-conductor grade, 10 % w/w) and pinched off. It is laid down and continuously rotated slowly for forty minutes. Furthermore, it is immersed in a hot bath (50 °C) for forty minutes with ultrasonic agitation (600W, 28KHz, 8unites). Then, the hydroperoxide is extracted from the cavity and disposed. The cavity is showered with demineralized water for ten minutes in order to remove hydroperoxide from the cavity inner surfaces.

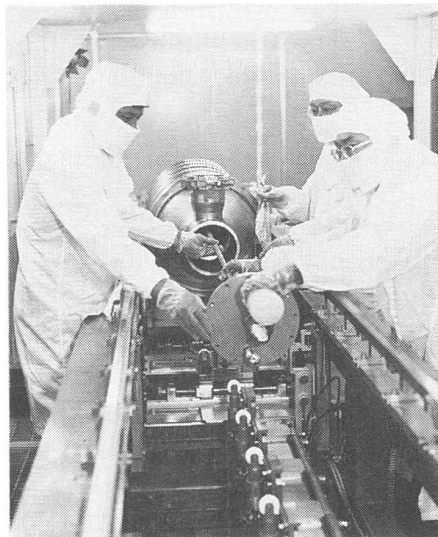


Fig.49
Extraction of cathode from five-cell cavity after first rinsing.

Third Rinsing

During the first and second rinsing, the demineralized water

is once stored in the tank. Thus, the quality of the water should drop. During the third rinsing, we use water directly coming from a pure-water system(Fig.50).

We set a shower pipe in the cavity and the pure water is poured to the cavity through it. The resistivity of the water is $9 \sim 10 \text{ M}\Omega \text{ cm}$. The cavity is immersed in a hot bath(50 °C) with an ultra-sonic agitator. Overflowing of the water is carried out for a long time.

Analysis of Rinsing Status

The overflowing time is determined as follows. In this system, the specific resistivity of the overflowing water decreases exponentially with time, as shown in Fig.51. We obtain a logarithmic equation from the fitting of the curve,

$$\rho(t) = \rho(0) \cdot \exp(-t/\tau) \quad (18)$$

From this equation, we can easily estimate the chemical residue (Cres) and the rinsing rate (Crate), as follows:

$$\begin{aligned} \text{Cres} &= \int_{t_0}^{\infty} \rho(t) dt \\ &= \tau \cdot \rho(0) \cdot [1 - \exp(-t_0/\tau)] \end{aligned} \quad (19)$$

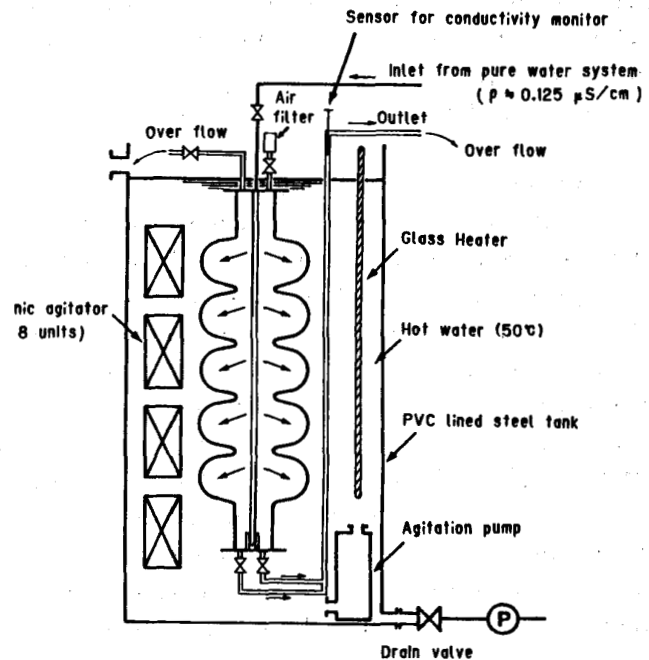


Fig.50
Third rinsing method.

$$\text{Crate} = \int_0^{t_0} \rho(t) dt / \int_0^{\infty} \rho(t) dt$$

$$= 1 - \exp(-t_0/\tau) \quad (20).$$

Here t_0 is the overflowing time. Because ultra-pure water rinsing after this rinse is a short time, we control the rinsing state by Cres and Crate.

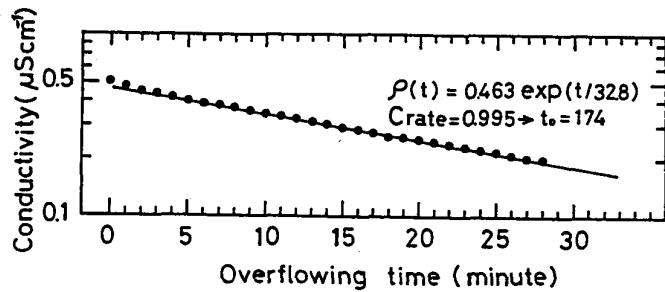


Fig.51

Time dependence of conductivity of the overflowing water in third rinsing.

Threshold Field of Field Emission

Figure 52 shows the correlation between chemical residue (Cres) and threshold field of field emission, which has been obtained from TRISTAN scc production. If the cavity has no material defects which cause breakdown, keeping the chemical residue to less than $0.1 \text{ sec} \cdot \mu\text{S/cm}$, one can hope to obtain a maximum accelerating field of 10 MV/m "without field emission".

We continue to overflow water until Crate becomes larger than 0.995. This takes 170 minutes. Finally, when we dump the water in the cavity, we introduce the nitrogen gas into the cavity. If not so, the resistivity drops to $5 \text{ M}\Omega \text{ cm}$ due to CO_2 gas in the air.

Ultra-pure water rinsing

As a final rinse, we carry out ultra-pure water rinsing ($\rho = 17 \sim 18 \text{ M}\Omega \text{ cm}$). Our demineralized pure water is high quality in resistivity, but it is not controlled for particles less than 10 microns, bacteria and TOC which can be a field emission source. We show the quality of our ultra-pure water in Table 4. The aim of ultra-pure water rinsing is to remove such substances from the cavity inner surfaces. We repeat overflowing and dumping of the ultra-pure water twice. It takes forty minutes. After this rinse, the cavity is filled with nitrogen gas and immediately sent to KEK from the company, traveling for about two hours.

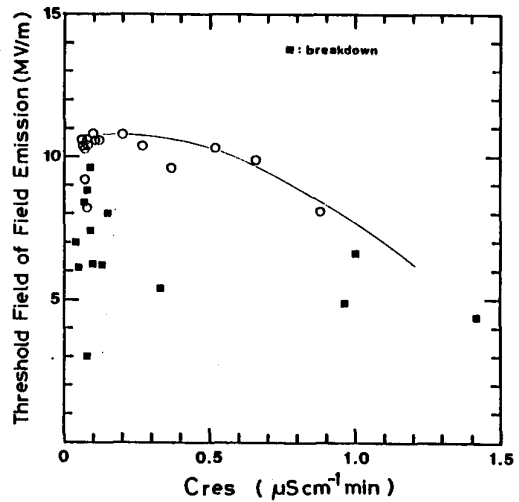


Fig.52

Correlation between chemical residue on the cavity inner surface and threshold field of electron field emission.

Tab.4
Quality of our ultra-pure water.

Terms	Sampling Date '87 7/21	Sampling Date '88 2/18	Guarantee Value
Particles ($\geq 0.2 \mu m$) piece/ml	16	19	≤ 50
Bacteria piece/ml	2.7	0	≤ 1
SiO ₂ (ppb)	12	25	≤ 50
TOC (ppb)	180	< 50	≤ 200
Resistivity (M Ω cm)	17.6	17.6	≥ 18

7-4 Pollution Problem of EP System

We could solve the problems of Qo-switching and field emission by the use of a fresh EP solution at EP-II and by improvements in rinsing method. However, the measure against system pollution was not perfect.

Accumulation of Pollution

As shown in Fig.53, we often observed pollutants at both end plates of the HR-EP system in EP-I. Also, in EP-II, we often found pollution at the inside of the rotary sleeves(Fig.54). Thus, some pollutants must be distributed and accumulated in the EP system. We had been watching when they again brought about problems.

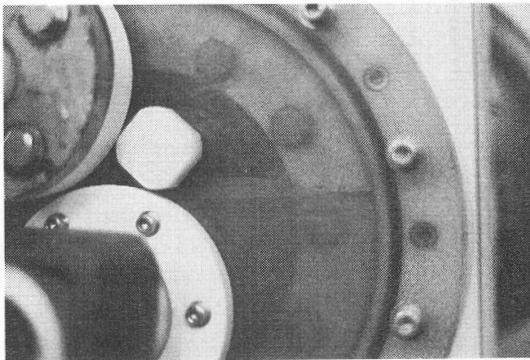


Fig.53
Pollution at the end plate of the horizontal EP system in EP-I.

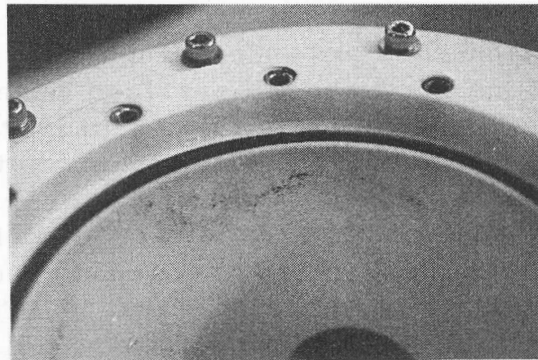


Fig.54
Pollution in the rotary sleeve after EP-II.

Occurrence of System Pollution

As shown in Fig.55, it came at 4a~5b cavities. Figure 55 suggests that something happened in our EP system. We decided to disassemble the EP system and to clean it. All parts such as the reservoir tank, tubing pipes, heat exchanger, and pumps were polluted with greenish-yellow matter. The pollutants were easily rubbed off with a cloth containing atheton. We gathered pollutant powder(9.4 g) from the bottom of the reservoir tank and analyzed it with EPM, FTIR and the extraction method. We could find some kinds of metal components(Al,Cr,Fe,Ca,Si) which were contained in the buffing abrasive. However, surprisingly, 85 percent of it was "pure sulfur". We started paying attention to sulfur since then. Sulfur gave us the chance to employ hydroperoxide rinsing, as

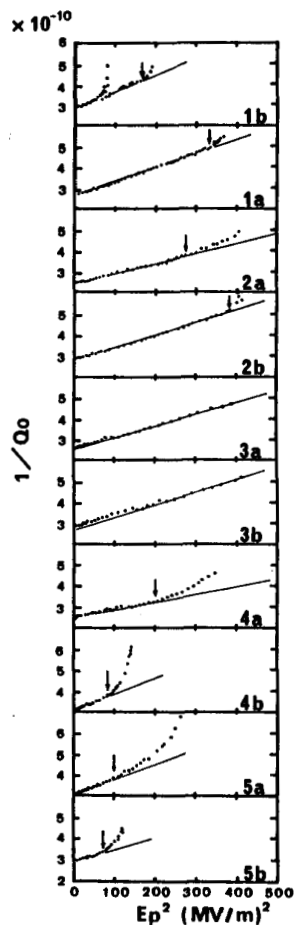


Fig.55 Occurrence of field emission in our mass production.

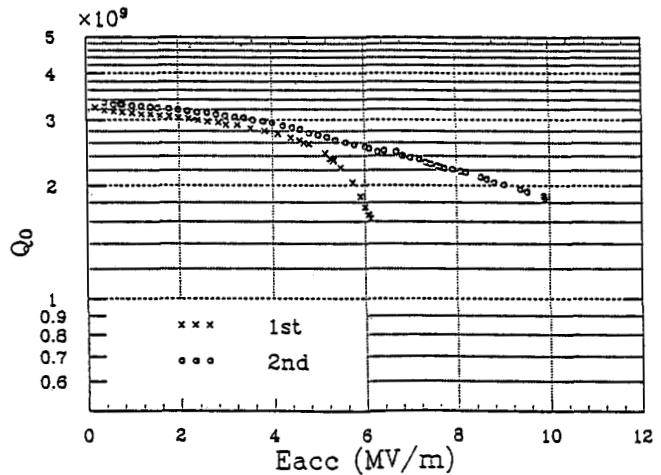


Fig.56 Improvement of sc performance by EP system cleaning.

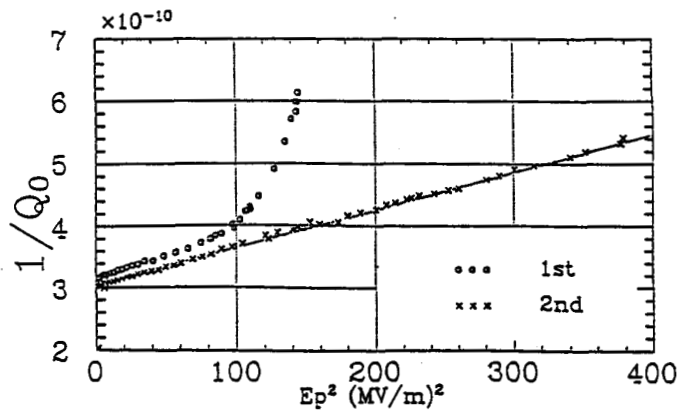


Fig.57 Improvement of the sc performance by EP system cleaning with field emission.

noted before. At that time, we did not think seriously that sulfur directly comes out by the decomposition of the EP solution, like in Fig.44. The amount of decomposition is a very little. By our estimation, 0.1 percent of the hydrogen generated during electropolishing reacts with sulfuric acid in the EP solution, and generates sulfur(2g) in each EP-I by a five-cell cavity. This kind of problem is peculiar to large-scale production.

Employment of Pre-EP

Sulfur contamination is a demerit in electropolishing, and is inevitable. However, sulfur is often found around metal components, as can be seen in Fig.44. This suggests that sulfur is easy to deposit around such a core. If buffing stains on the cavity surface are few, it would be somewhat difficult for sulfur to deposit. By sample tests, it was found that the buffing abrasive left on the niobium surface can be removed by EP of 2μ m. We have additionally introduced Pre-EP in order to remove the buffing abrasive left on the cavity inner surface. Namely, before EP-I, we electropolish the cavity by $3\sim 4\mu$ m with the stored EP solution in the cavity. The solution is not circulated. After Pre-EP, the solution is disposed. Buffing stains should go out with the solution. In the fabrication process outlined in Table 2, (7) was added from the 7a cavity. This measure was a tentative one, but we decided to continue watching for a while. It was fortunate for us that since then such a problem has not occurred to the end of TRISTAN scc production.

Improvement of SCC RF Performance by System Cleaning

The maximum fields of cavities 4b and 5b were 6.1 and 5.6 MV/m, respectively, in the first vertical tests. After cleaning the EP system, we retreated them. As shown in Figs.56 and 57, the performance of cavity 4b improved and the maximum field reached 10 MV/m without field emission. Cavity 5b quenched again. The maximum field did not change so much (5.8 MV/m). The cause of quenching is suspected to be an EBW defect because, as described in 7-6, the quenching had neither a heavy field emission nor heavy heating (fast quenching).

7-5 Quenching Due to Material Defects

In the first vertical tests, two cavities (6a,13b cavities) quenched at the accelerating field lower than 5 MV/m, which is our operation target value. These cavities were diagnosed with temperature mapping.

Measurement of Qo-Eap Curves in Side Bands

We have no well-developed diagnosis system as do other laboratories [14] . When a cavity is quenched, we measure the "Qo-Eap" curves of the side bands besides the fundamental mode (π - mode). The achievable maximum axial peak fields(Eap) in the side bands are affected by which cell has a quenching source. We show the calculated field distributions for each mode excited in our five-cell cavity in Fig.58. Eap will be higher than that of the fundamental mode in the side band, which excites a weak magnetic field in the quenching cell. On the other hand, it is the same as that of fundamental mode in the side band, which excites a strong field in the quenching cell. Figure 58 shows an example(6a cavity) of Qo-Eap curves whose quenching source is in the center cell. However, in each mode the field distribution is symmetric with the center cell; thus this method can not be used to determine whether the source is in one of the end cells, except for the center cell. Nevertheless, it can be solved by attaching one carbon resistor to each cell.

Temperature Mapping System at KEK

After guessing which cell has the quenching source in this

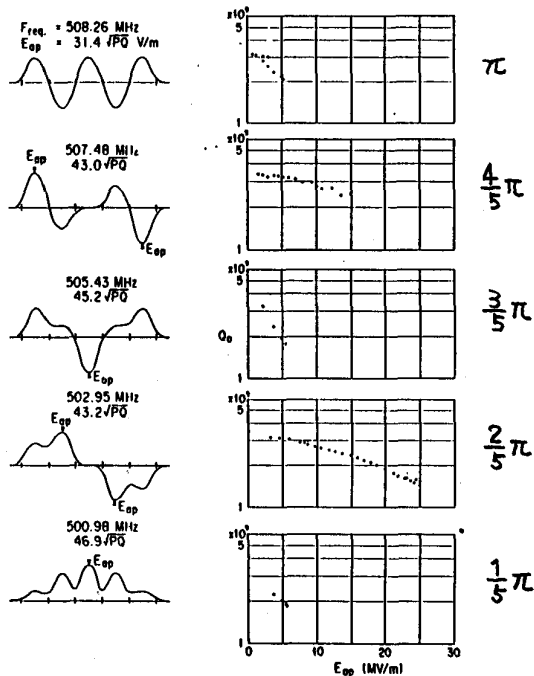


Fig.58
Field distribution and
Qo-Eap curves for side
bands.



Fig.59
Heat-mapping system at
KEK(for 13b).

way, we attach 384 carbon resistors to the corresponding cell. The place resolution is 3.5 cm. Measuring the cavity again, we found the quenching region by temperature-mapping. Figure 59 shows our temperature-mapping system for the cavity 13b. Unfortunately, in this case, the quenching source was on the iris EBW seam of an end cell. An ally of resistors thus had to be attached to two cells.

Material Defect

We show a photograph of the defect at the center cell of 6a in Fig.60. It was 3 cm away from the equator EBW seam. It appeared to be a fissure of the λ character by visual inspection. The size was about 8 cm. Upon the inspection after EP-I, it was not found; it would thus appear in EP-II. Figure 61 shows heat-mapping after the first grinding. By the grinding of 40 ~ 90 μ m of the dashed area and EP-II the Eacc was little improved. Again, the area was ground off by 300 μ m; it then increased to 7.6 MV/m.

Cavity 13b was ground so as to remove all suspicious parts by inspection after side-band measurement. Therefore, we do not know which was the quenching source; after the grinding, however, the quenching source still remained on the iris EBW of an end cell. It limited the Eaccmax to 8.4 MV/m by the fast quenching(see 7-6).

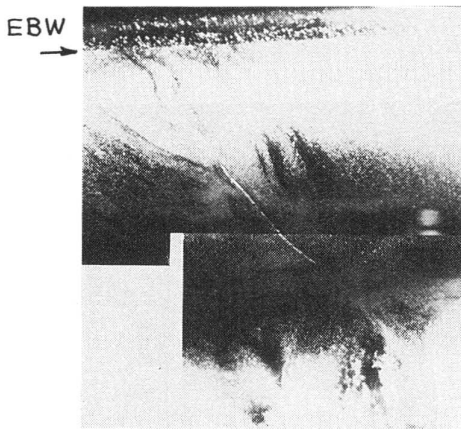


Fig.60
Photo of the defect area in 6b.

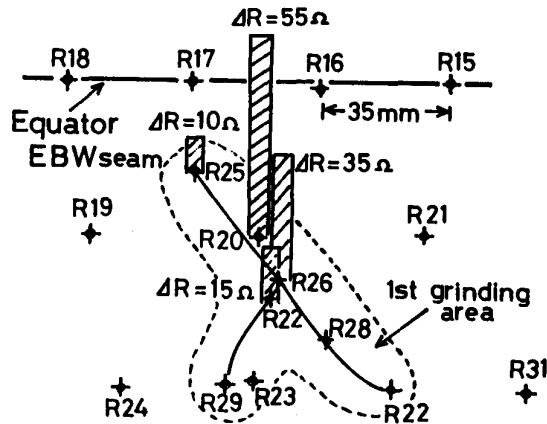


Fig.61
Temperature mapping of the defect area in 6b after first grinding.

7-6 Performance of TRISTAN SCC

Distribution with Maximum Field Gradients

In Fig.62 we show the statistics of the maximum accelerating

field in the first vertical tests. It has two peaks: one is at around 8 MV/m, the other around 10 MV/m. The former shows mainly the quenched field distribution.

In our vertical test, at fields higher than 10 MV/m, the cavity wall losses become 200~400 W. Then, the pressure rising in the cryostat due to helium boiling occurs rapidly. In such a condition the measurement becomes difficult. In addition, at such high fields, the input power is so much that the N-connector, which connects the input cable at the cryostat, is heated up. It often broke down at input power of 300~400 W. These two reasons limit measurements to around 10 MV/m. Thus, the distribution around 10 MV/m has no meaning.

Our Industrial Technical Level

Figures 62 and 63 show our present technical level. Figure 62 shows the results after retreatment. Eight cavities were retreated. Among them, four cavities were reworked for repairing, which are dotted in the figure. The other four cavities were retreated due to problems with the input couplers. It shows that we can control the accelerating field of 7 MV/m with retreatments. The average achievable accelerating field was

$$E_{accmax} = 9.6 \pm 1.4 \text{ MV/m}$$

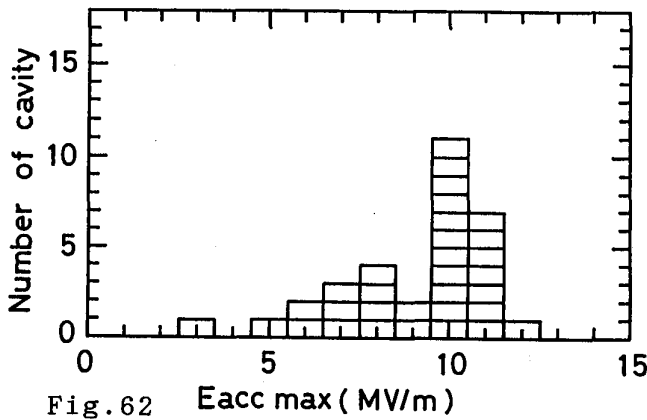


Fig.62 Distribution of the maximum achievable field gradients of thirty-two five-cell TRISTAN sec at the first vertical tests.

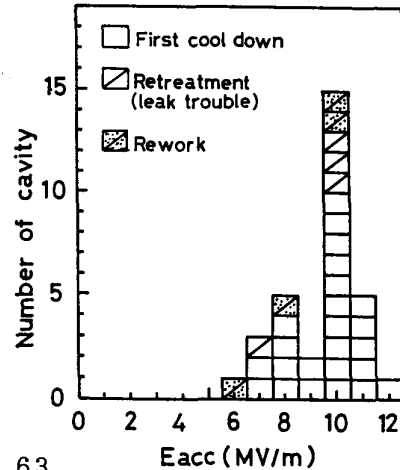


Fig.63 Distribution of the maximum achievable field gradients after retreatment.

for results after retreatments. The yield rate in the first cold test was

$$Y = 100 \times 28/32 = 88 \%$$

Classification of Q₀-Eacc Curves

We show typical Q₀-Eacc curves of the TRISTAN scc in Fig.64. They are classified into four groups, as shown in the figures.

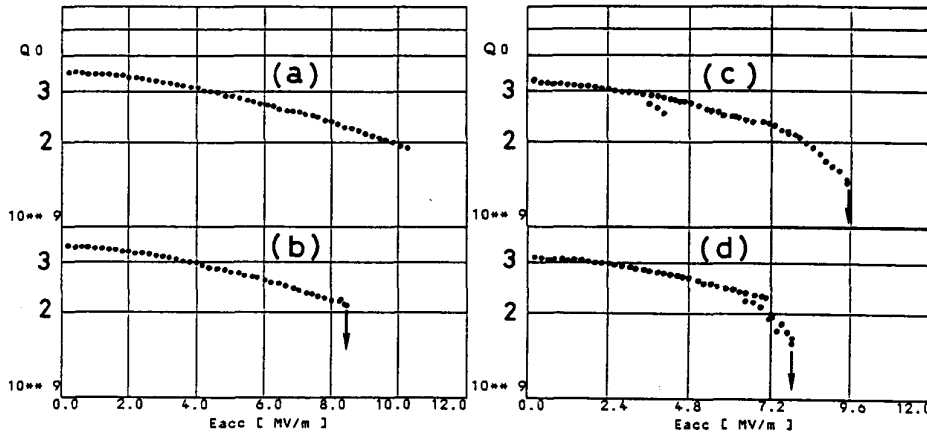


Fig.64
Typical Q₀-Eacc curves of TRISTAN scc
classified into four group.

- (a) Without heavy field emission to 10 MV/m . . . 22 cavities.
- (b) Fast quenching 7 cavities.
- (c) Quenching after field emission 2 cavities.
- (d) Q₀-switching 1 cavity.

In order to obtain 10 MV/m, we must overcome fast quenching around at 8 MV/m. For such quenching sources, defects on EBW seams (like cavity 13b) are suspected. As can be seen in Fig.64, fast quenching involves neither large heating nor heavy field emission. It looks like magnetic quenching. We therefore guess that it is due to some low-H_c(about 300 Gauss) weak superconductors.

Distribution with Q₀ Values

Figure 65 shows statistics regarding the Q₀ values at 5MV/m of TRISTAN scc in vertical tests. The average value is

$$Q_0(\text{ at } 5 \text{ MV/m }) = 2.8 \pm 0.2 .$$

The variation is about 10 percent. As shown in Fig.66, the RRR of the cavities was scattered about ten percent,

$$RRR = 152 \pm 17.$$

The Q_0 variation, partially, comes from this scattering.

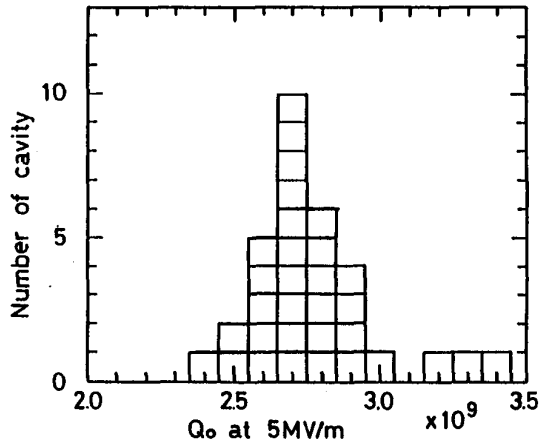


Fig.65
 Q_0 distribution at 5 MV/m
 in vertical tests for TRIS-
 TAN thirty-two cavities.

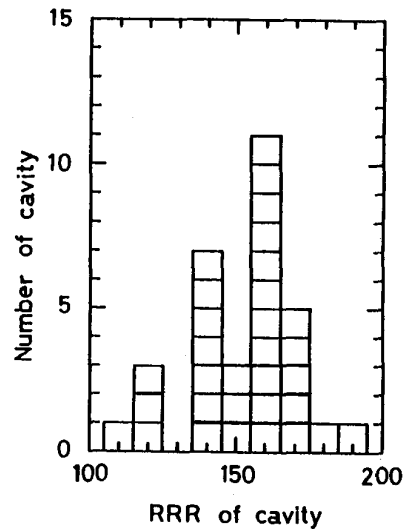


Fig.66
 Distribution of RRR
 of TRISTAN scc.

Estimation of Residual Surface Resistance

According to BCS theory, BCS surface resistance of a sc cavity increases with RRR value, because the increase of RRR makes the non Cooper-paired electron mean free path long [15] . Figure 67 shows the correlation between RRR and inverse Q_0 . As presented in eqs.(7) and (8), if R_{res} is small, inverse Q_0 is proportional to R_{BCS} . A coarse tendency that inverse Q_0 increases with RRR can be seen. Our average surface resistance(R_s) value at a low field of thirty-two cavities is

$$R_s = 80 \text{ n}\Omega$$

at 4.2 K. According to reference [15] , the non Cooper-paired electron mean free path l is given as

$$l = 20\text{\AA} \times RRR, \tag{21}$$

and the BCS surface resistance ratio is

$$R_{BCS}(l)/R_{BCS}(1000 \text{\AA}) \sim 1.28. \tag{22}$$

for $l = 3000 \text{\AA}$. Here, a mean free path of $l = 1000 \text{\AA}$ corresponds to a RRR value of 50, by eq.(21). If we take the value of $R_{BCS}(l=1000 \text{\AA})$ from our experimental value at 4.2 K [16] , it is

58 nΩ (Rres=7.8nΩ). It was measured with the first 500-MHz single-cell cavity with RRR= 40. From these values, estimating the average RBCs of the TRISTAN scc is as follows

$$R_{BCs} = 1.28 \times 58 = 74 \text{ n}\Omega .$$

From this value, we can estimate our average Rres is,

$$R_{res} = 80 - 74 = 6 \text{ n}\Omega .$$

This value is the same as that of the single-cell cavity. This means uniform polishing of each cell in a five-cell cavity.

Degradation of SCC RF Performance in Pair Assembly Process and in Operation

At last, we briefly mention the performance in horizontal tests and MR operation. Details are described in other papers [17] . Figure 68 shows changes in the Eaccmax in horizontal tests and after the operation of 3100 hrs in MR, for the first sixteen TRISTAN scc. One can see that the Eaccmax dropped from 10 to 7 MV/m after the horizontal tests. As shown in Fig.70, the recent studies on nitrogen gas or air exposure for 24 hours showed little influenced on the scc RF performance. This degradation might be due to dust particles which enter during horizontal

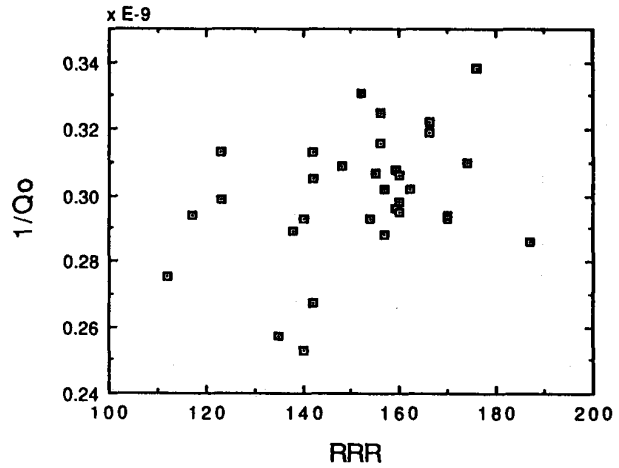


Fig.67
Correlation between inverse Qo and RRR of cavities.

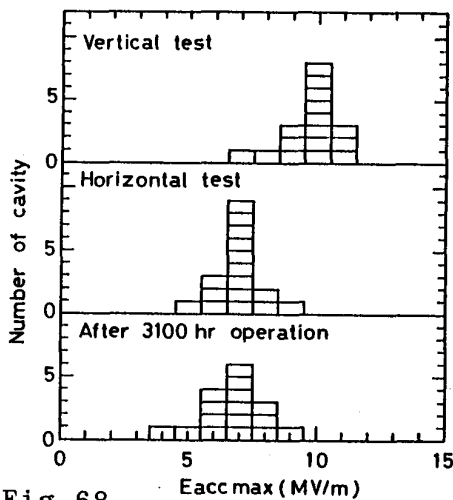


Fig.68
Change of Eacc max from vertical test to after 3100 hrs operation.

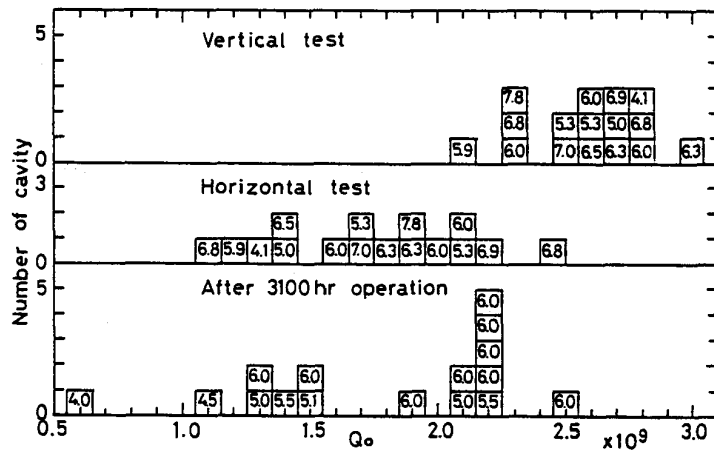


Fig.69
Change of Qo from vertical test to after 3100 hrs operation.

assembly or when the input couplers are set to the cavities. However, during the 3100 hours dedicated to physics runs, the Eaccmaxs have so far been stable.

Figure 69 is the same figure for Q_0 values. The number in the box means the accelerating field at which Q_0 values were measured. After horizontal tests, the Q_0 values scattered widely. So far, the large changes in the Q_0 values are not found in operation, except for one cavity.

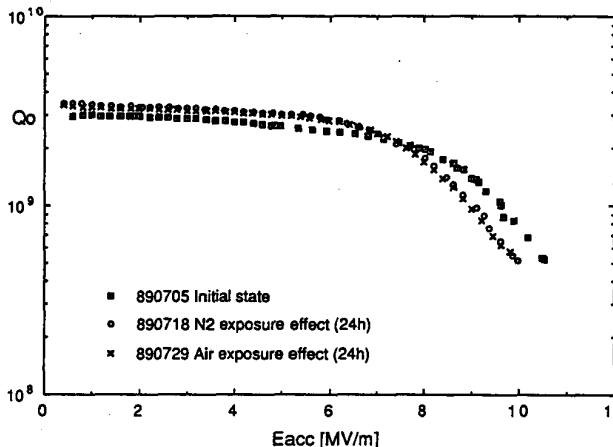


Fig.70
Effect of nitrogen gas and air exposure for 24 hrs.

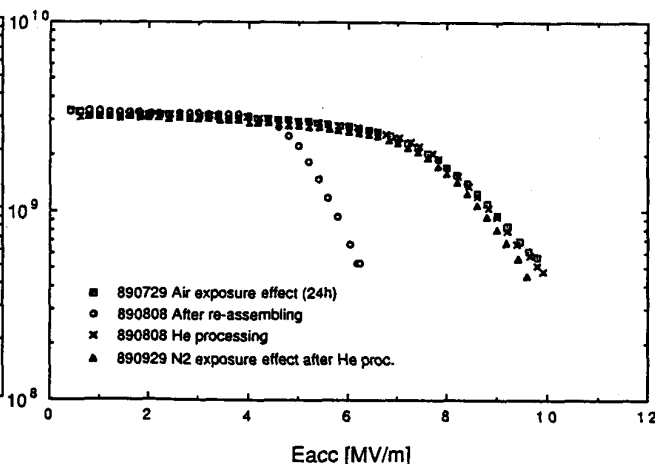


Fig.71
Effects of helium processing and its nitrogen gas exposure(24 hrs) on scc RF performance.

8. Future plan

In the future we will start a feasibility study on the application of scc to a linear collider, B physics, and free electron laser.

8-1 Two Problems in Cavity Fabrication

In order to upgrade the accelerating field of the scc, regarding cavity fabrication we must solve the following problems:

- (1) Fast quenching at 7~ 8 MV/m.
- (2) Q_0 -switching or field emission.

Fast quenching would mainly be caused by defects with low- H_c weak superconductors(magnetic quench). This kind of problem can not be solved by the use of higher thermal conductivity niobium

materials, since it is not the thermal instability phenomenon but the magnetic one.

Improvement in EBW

Fast quenching had been experienced during the initial stage of developing 500-MHz single-cell cavities. Such defects were often on EBW seams at equators. Thus, we suspect EBW seams as being the cause of such defects.

We are now able to apply rhombic raster EBW as a result of extensive studies. However, this method was applied to the equator EBW of only some TRISTAN sc cavities. All irises of the TRISTAN scs were welded using a defocused electron beam. In order to establish 10-MV/m cavities, it is necessary to improve EBW.

Development of Inspection Equipments

We experienced quenching due to material defects (6a cavity). Secondly we suspect material defects as being the cause of fast-quenching. To solve them, one way is to more strictly control the fabrication process of niobium material. However, it is the best way to introduce a reliable inspection to niobium sheet materials or half cells. Although, today, many laboratories have introduced some kinds of checking, such as an anodization-check or visual check, they are insufficient by themselves. As experienced in cavity 6a, material defects are often contained in the niobium matrix. We need information concerning the 50~100 microns depth. An anodization-check or a visual check can not result in such information. At present, no commercial equipment is available for such an inspection. We must develop some equipment for such inspections. A non destructive inspecting device using scanning laser acoustic microscopy, which has been developed by M.G Oravec et al. [18], may be useful for this purpose.

Measures against Sulfur

The second problem would be caused by surface contamination by sulfur. The generation of sulfur in niobium electropolishing is inevitable. In Fig.72, we illustrate sulfur generation during EP. About 4 mg/L is generated by each EP-I (80 μ m) for a five-cell structure. In order to solve this problem, the best methods would be as follows:

- (1) To separate the EP system into two parts, one for EP-I and the other for EP-II.
- (2) Setting filters in each system in order to remove pollutants.
- (3) Removing the sulfur which adhered on the cavity inner-

surface during EP-I by dissolving it with CCl_4 , CS_2 or acetone.

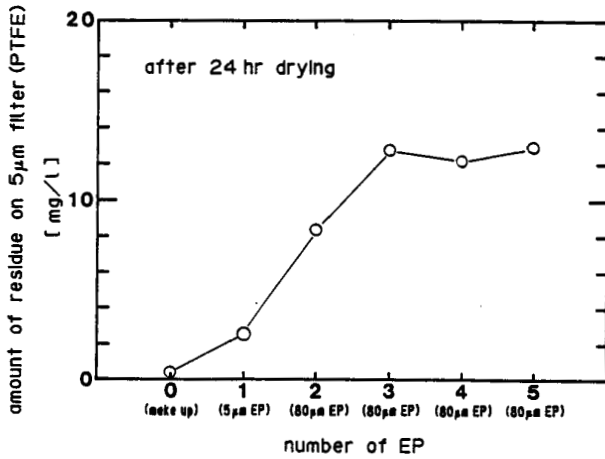


Fig.72 Accumulation of sulfur in an EP system.

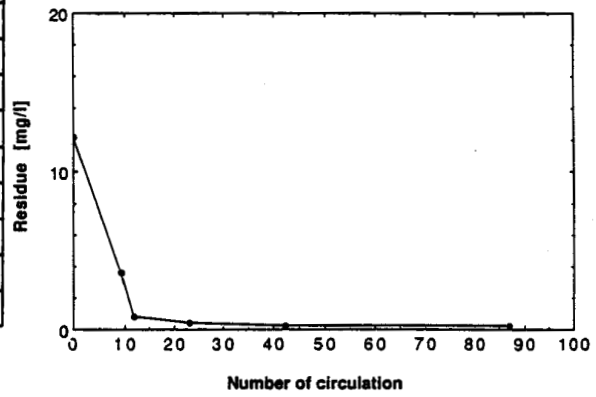


Fig.73 Filtering effect by active carbon.

Recent Studies on Measures Against Sulfur

We are now studying how to solve this sulfur problem for future high accelerating field cavities. Figure 73 shows the results when we filtered the polluted EP solution with active carbon and a teflon filter(10 µm). It means that if one circulates the EP solution through filters about 30 times, most of the pollutants can be removed.

Figure 74 shows the surface contamination of the niobium samples which were electropolished with the filtered EP solution. In the case of a polluted EP solution, the heavy carbon contamination was found. On the other hand, it was only little in the case of filtered EP solution and was near to that of fresh EP solution. It shows an encouraging result for active carbon filtering method.

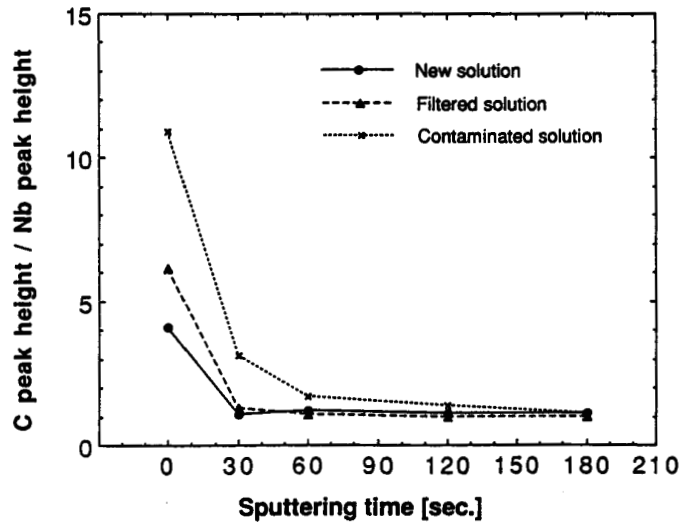


Fig.74 Filtering effect on polished surface contamination.

8-2 Degradation of SCC RF Performance in Cavity Pair Assembly

In addition to the above-mentioned in fabrication problems, we have another practical problem concerning assembly before the insertion into a horizontal cryostat. As noted before, the Eacc degraded from 10 to 7 MV/m after assembly. The Q_0 values also degraded. It would be mainly caused by dust particles during assembling. We used the class-100 clean room for connecting two cavities and attaching HOM couplers. However, the work of mounting input couplers on the paired cavity in a cryostat is done in a non-clean environment. Though careful measures are taken regarding it, they might be insufficient.

Performing of Helium Processing in Horizontal Test

In order to solve the above-mentioned problem, we have to reconsider this assembling process. However it may be better to perform helium processing in a horizontal test. Since the sparking trouble described in 2-2, we have not carried out helium processing for five-cell structures. We have been afraid of sparking at the input coupler. In addition, we have thought that it is difficult to do helium processing in an accelerator. However, we recently obtained results which make such thoughts change. Figure 71 shows the results. To check which assembly process degrades the scc performance, we reassembled a single-cell cavity in the clean room and measured it. Unfortunately, we then suffered a leak at the indium sealing at the beam pipe flange. Some dust particles may have entered the cavity. The Eacc degraded from 10 to 6 MV/m. Any RF processing seemed to be ineffective. Subsequently, we performed helium processing for 45 minutes. The scc RF performance was completely recovered. After this measurement, it was exposed to pure nitrogen gas for 24 hours and measured again. We confirmed that the helium-processed surface is not affected by at least 24 hours nitrogen gas exposure. We can hope for TRISTAN scc to recover the performance by light helium processing in a horizontal test.

8-3 Niobium Coated Cooper Cavity

In the near future, we will start R & D on a higher accelerating field gradient with niobium cavities. It is also a fundamental problem how cheaply to construct sc cavities. A niobium-coated copper cavity seems to be promising for this reason [19] . We have just started to study it with L-band cavities [20] , and are now assembling a new measurement system for them.

9. Conclusions

As presented by D.Bloess in the third workshop at ANL, there are only four rules regarding surface treatment for sc cavities [21] :

1. Clean materials (highly pure niobium without inclusions).
2. Clean polishing chemicals and solvents.
3. Ultraclean rinsing water.
4. Ultraclean assembly environment.

However, in practice to know the rules much experience is required in order to understand what to do concerning them. Troubles were caused from unexpected facts. We often concretely understand how we should do according to the rules in our struggle with the troubles. In this paper, we boldly described the problems that we have encountered and how we have solved them for the TRISTAN scc. Our experiences in R & D and TRISTAN scc production allow the following conclusions.

9-1 Hydrogen Problem in Electropolishing

We experienced two kinds of hydrogen problems in electropolishing.

Heavy Hydrogen Absorption

One is much hydrogen absorption by niobium during heavy electropolishing, which has been well known [22] . This gives a large degradation, with a Q_0 value of two orders of magnitude. However, it can easily be improved by annealing at temperatures higher than 700 °C.

Grooving of Surface by Hydrogen Gas

The other problem was the grooving of the cavity inner surface by hydrogen gas bubbles during vertical electropolishing for a three-cell cavity. This effect degraded the Q_0 value by several times. This problem was solved by using horizontal rotational electropolishing.

9-2 Surface Contamination

We met the three kinds of surface contamination problems.

System Materials

The first was surface contamination by dissolving the materials of the surface treatment equipment to an EP solution.

They led to a Q_0 value degradation or heavy field emission. To eliminate the problem, great care must be taken in the selection of materials for surface treatment. Recommended materials for an EP system are Teflon(PTFE, PVD, PFA) and polyethylene(PE). It is better not to use Viton, as possible as.

Buffing abrasive

The pollution of an EP solution by a buffing abrasive material was suggested by Dr. Bloess in the 2nd SC-RF workshop [10] . In our process, since buffing is carried out for all inner surfaces of half cells, it became a serious problem. It often leads to Q_0 -switching or heavy field emission on scc RF performance. In order to solve the problem, one has to remove them from the surface before heavy electropolishing.

Sulfur

EP solution contamination by sulfur is inevitable as long as one employs electropolishing. Not to suffer the problem, one has to use a fresh EP solution during the final electropolishing. Filtering of the EP solution using active carbon may be useful as a measure against pollution.

9-2 Development of EP System

Although a number of disadvantages with EP are discussed in the reference [10] , we have believed that a smoothly polished surface and easy control of polishing (no run-away reaction) with EP should have beneficial effects on scc RF performance or quality control of polishing.

As described in section 3, by great efforts with EP, we could improve many of the disadvantages and have completed a highly reliable EP system(HR-EP). By using this system with the TRISTAN scc we obtained a high yield rate of 88 % during the first cold tests. Furthermore, it has to be emphasized that field emission is only a small problem in our cavities. It has been shown that as for scc RF performance and quality control, electropolishing was a good choice as the scc surface treatment method of large-scale production.

9-3 Importance of Rinsing

We discussed the importance of rinsing after the final treatment. In addition to ultra-pure water rinsing, long-time rinsing with highly pure water(10 M Ω cm) is important against field emission. Especially, it has to be emphasized that one should use a monitor for dumped water and has to judge the rins-

ing status of the cavity.

9-4 High Thermal Conductivity Niobium Material.

We developed a high thermal conductivity niobium material by combining the making of high-pure niobium ingots by multi-melting with titanium wrapped annealing. Its use had an important role in increasing the Eacc of TRISTAN scc up to 10 MV/m. In addition, by suppressing the Q_0 dropping by surface heating, it contributed to the high Q_0 value at high fields.

9-5 TRISTAN SCC

TRISTAN scc was the first large scc project involving the storage ring. In this production we have obtained an Eacc of 9.6 MV/m and a Q_0 value at 5 MV/m of 2.8×10^9 "on the average" in vertical tests. We have established an industrial fabrication method for scc large-scale applications. We can control the Eacc of 7 MV/m by the fabrication method. To control an Eacc of higher than 10 MV/m, we will have to solve the problems of the magnetic quenching and sulfur contamination in EP. To increase the yield rate in the production, a reliable non-destructive inspection system which can detect information at 100-microns depth of the niobium matrix should be developed.

We experienced degradation of 30 % in scc RF performance during the assembly of a paired cavity and cryo-module. It should be emphasized that input couplers also must be attached to the cavities in clean environments as in cavity-connecting assembly. Furthermore, one has to take care not to bring dust particles into the cavity from input couplers. As a recovering measure against the degradation of scc performance, helium processing in the horizontal test may be effective.

So far, no large degradation of performance has been seen during 3100 hours of operation. The first sixteen cavities have been operated on the average Eacc of 4.4 MV/m.

Acknowledgments

The authors would like to thank former Director T.Nishikawa, Director H.Sugawara, Professors S.Ozaki and Y.Kimura for their continuous encouragements.

We also would like to express our thanks to other KEK peoples who helped us. Dr. Y.Kanda and Mr. M.Taira (Chemical division) greatly contributed with the analysis of polluted EP

solutions. Mr. H.Abe and Y.Ajima(Machine shop division), they have contributed with the fabrication of 1.5-GHz dividable single-cell cavities in spinning and electron beam welding. Dr. M.Wake and Mr. K.Mimori(Cryogenic division), they kindly supplied liquid helium for our RRR measurements.

We are grateful to Dr. K.Yoshihara and Mr. M.Tosa of National Research Institute for Metals. They have kindly provided their degasing analysis system and surface analysis equipment (Auger,ESCA) and helped us.

Many of these studies were carried out in close collaboration with Nagoya Aircraft works in Mitsubishi Heavy Industries, Ltd., Nomura Plating, Co., Ltd., and Tokyo Denkai, Ltd.

We are grateful to the people of Nagoya Aircraft works. Mr. K.Tajiri, M.Jinno and K.Moewaki contributed greatly with studies of refreshing EP solutions. We are pleased to acknowledge to Mr. T.Sawada and Y. Nomaru for their considerable assistance with analysis(FTIR, Gas Chromatography) of the polluted EP solutions and surface analysis (EPM). Mr. S.Hamai and Y.Sugiura contributed a lot concerning the development of niobium material.

We are also deeply indebted to people at Nomura Plating, Co.,Ltd. We would like to thank Mr. S.Ohgushi, T.Ikeda and K. Ueno for their helpful suggestions and continuous encouragement. Mr. Y.Nishiyama and M.Nishigaki contributed with the design and construction of the horizontal rotational electropolishing system. Mr. H.Yoshida, H.Miwa, T.Suzuki and S.Fukuda have shared failure and success in these developments of surface treatment with us. They are now specialists on surface treatment of niobium sc cavities. H.Miwa and T.Suzuki had visited KEK for two years and helped us with other work, such as RRR measurements. We would like to thank them for their great contributions to KEK.

We would also like to thank Mr. Y.Yano, H.Otsubo, T.Tamura, M.Nishizuka, K.Teranishi and Y.Kosaka(Mitsubishi Heavy Industries, Kobe and Yokohama) for their help in cavity assembling for vertical tests.

The authors wish to express their thanks to Mr. Yuji Kojima, T.Ogitsu, K.Hara of our scc group for their supply of liquid helium for vertical tests. We are also grateful to Professor E.Ezura and Dr. K.Akai for building up the measurement system for vertical tests. Finally, we would like to thank other members of our scc group for their help and encouragement.

References

- 1) T.Furuya, S.Hiramatsu, T.Nakazato, P.Kneisel, Y.Kojima and A.Takagi ; IEEE Trans. Nucl. Sci. NS-28 No.3(1981)3255.
- 2) S.Noguchi, T.Furuya, K.Hara, K.Hosoyama, Y.Kojima, S.Mitsunobu, T.Nakazato and K.Saito ; Proc. 5th Symp. on Accelerator Science and Technology, KEK(1984). P.124.
- 3) T.Furuya, K.Hara, K.Hosoyama, Y.Kojima, S.Mitsunobu, S.Noguchi, T.Nakazato and K.Saito ; Proc. 5th Symp. on Accelerator Science and Technology, KEK(1984). P.122.
- 4) H.Padamsee ; Proc. 2nd Workshop on RF Superconductivity, CERN (July 1984), P.339.
- 5) H.Diepers, O.Schmidt, H.Martens and F.S.Sun ; Phys. Lett. 37A(1971), P.139.
- 6) P.Kneisel ; Proc. Workshop on RF Superconductivity (Karlsruhe,1980), P.27.
- 7) K.Tajiri, M.Jinno, K.Inoue, Y.Kojima, K.Saito and H.Nomura. ; Proc. 12th LINER ACCELERATOR MEETING IN JAPAN, JAERI(August 1987).
- 8) H.Diepers and O.Schmidt ; Japanese patent official report (Shyowa 55-39640) ; P.229(1980).
- 9) H.Padamsee ; IEEE Trans. MAG-19(1983), P.1308.
- 10) D.Bloess ; Proc. 2nd Workshop on RF Superconductivity, CERN(July 1984), P..409.
- 11) K.Asano, T.Furuya, Y.Kojima, S.Mitsunobu, H.Nakai, S.Noguchi, K.Saito, T.Tajima, M.Tosa and K.Yoshihara ; KEK Report 88-2, 1988.
- 12) T.Tajima, T.Furuya, T.Suzuki and Y.Iino ; "Pre-tuning of TRISTAN Superconducting RF Cavities" in this workshop.
- 13) E.Chiaveri ; CERN/EF/RF 89-1, 28 February 1989.
- 14) H.Piel ; Proc. the Workshop on RF Superconductivity, KfK(July 1980), P.85.

- 15) F.Palmer ; Proc. 3rd Workshop on RF Superconductivity, ANL(September 1987), P.309.
- 16) Y.Kojima, T.Furuya and T.Nakazato ; Jpn. J. Appl. Phys. 21(1982). P.86.
- 17) S.Noguchi, K.Akai, E.Kako, K.Kubo, T.Shishido and T.Suzuki; Proc. 14th Int. Con. on High Energy Accelerators, Tsukuba, Japan(August 1989)
- 18) M.G. Oravec, B.Y. Yu, K.Riney, L.W. Kessler and H.Padamsee ; Proc. 3rd Workshop on RF Superconductivity, ANL(September 1987), P.681.
- 19) C.Benvenuti, D.Bloess, E.Chiaveri, N.Hilleret, M.Minestrini and W.Weingarten ; Proc. 3rd Workshop on RF Superconductivity, ANL(September 1987) P.445.
- 20) K.Saito, S.Noguchi, S.Mitsunobu, M.Okuda, T.Otani and T.Suzuki ; Proc. 14th LINEAR ACCELERATOR MEETING IN JAPAN, Osaka Uni.(September 1989), P.231 in Japanese.
- 21) D.Bloess ; Proc. 3rd Workshop on RF Superconductivity, ANL(September 1987), P.359.
- 22) S.Isagawa ; Doctor thesis, Tokyo University(1979).